

# Innate lymphoid type 2 cells sustain visceral adipose tissue eosinophils and alternatively activated macrophages

Ari B. Molofsky,<sup>3,4</sup> Jesse C. Nussbaum,<sup>2,3</sup> Hong-Erh Liang,<sup>1</sup>  
Steven J. Van Dyken,<sup>1,3</sup> Laurence E. Cheng,<sup>5</sup> Alexander Mohapatra,<sup>3</sup>  
Ajay Chawla,<sup>2,6</sup> and Richard M. Locksley<sup>1,2,3</sup>

<sup>1</sup>Howard Hughes Medical Institute, <sup>2</sup>Departments of Medicine, <sup>3</sup>Microbiology and Immunology, <sup>4</sup>Laboratory Medicine, <sup>5</sup>Pediatrics and <sup>6</sup>Physiology, University of California, San Francisco, San Francisco 94143

**Eosinophils in visceral adipose tissue (VAT) have been implicated in metabolic homeostasis and the maintenance of alternatively activated macrophages (AAMs). The absence of eosinophils can lead to adiposity and systemic insulin resistance in experimental animals, but what maintains eosinophils in adipose tissue is unknown. We show that interleukin-5 (IL-5) deficiency profoundly impairs VAT eosinophil accumulation and results in increased adiposity and insulin resistance when animals are placed on a high-fat diet. Innate lymphoid type 2 cells (ILC2s) are resident in VAT and are the major source of IL-5 and IL-13, which promote the accumulation of eosinophils and AAM. Deletion of ILC2s causes significant reductions in VAT eosinophils and AAMs, and also impairs the expansion of VAT eosinophils after infection with *Nippostrongylus brasiliensis*, an intestinal parasite associated with increased adipose ILC2 cytokine production and enhanced insulin sensitivity. Further, IL-33, a cytokine previously shown to promote cytokine production by ILC2s, leads to rapid ILC2-dependent increases in VAT eosinophils and AAMs. Thus, ILC2s are resident in VAT and promote eosinophils and AAM implicated in metabolic homeostasis, and this axis is enhanced during Th2-associated immune stimulation.**

## CORRESPONDENCE

Richard M. Locksley:  
locksley@medicine.ucsf.edu

Abbreviations used: AAM, alternatively activated macrophage; HFD, high-fat diet; ILC2, innate lymphoid type 2 cell; iNKT, invariant natural killer T cell; ND, normal diet; SVF, stromal vascular fraction; VAT, visceral adipose tissue.

Diverse immune cells participate in the regulation of visceral adipose tissue (VAT) and metabolic homeostasis. With obesity, pro-inflammatory macrophages, neutrophils, CD8<sup>+</sup> T cells, CD4<sup>+</sup> Th1 cells, and mast cells accumulate in VAT and contribute to local and systemic inflammation, ultimately promoting insulin resistance and the development of metabolic syndrome and type 2 diabetes; in contrast, normal lean VAT contains eosinophils, alternatively activated macrophages (AAM), invariant natural killer T cells (iNKTs), and regulatory T (T<sub>reg</sub>) cells that can promote insulin sensitivity and metabolic homeostasis (Chawla et al., 2011; Schipper et al., 2012; Wu et al., 2011). How lean, healthy VAT recruits and sustains these distinct immune cell types remains largely unknown.

We previously reported that eosinophils reside in VAT and that eosinophil deficiency impairs Arginase-1<sup>+</sup> AAM accumulation. VAT eosinophils are abundant in IL-5 transgenic mice and promote AAM accumulation and insulin sensitivity (Wu et al., 2011; Chawla et al., 2011).

Prolonged VAT eosinophilia after helminth infection is also correlated with improved metabolic parameters in animals challenged with high-fat diet (HFD; Wu et al., 2011). Eosinophil production, bone marrow release and tissue recruitment and retention depend on several cytokines, chemokines, and integrins. IL-5 is integral at multiple levels, promoting eosinophil bone marrow production, release, and tissue recruitment, and is required for optimal systemic and local eosinophilia in diverse models of allergic inflammatory responses (Mould et al., 1997; Kopf et al., 1996; Foster et al., 1996). In contrast, IL-5 deficiency in unperturbed animals leads to a modest reduction in bone marrow, blood, and gastrointestinal tract eosinophil levels, indicating eosinophil production and recruitment to certain tissues can occur

© 2013 Molofsky et al. This article is distributed under the terms of an Attribution-Noncommercial-Share Alike-No Mirror Sites license for the first six months after the publication date (see <http://www.rupress.org/terms>). After six months it is available under a Creative Commons License (Attribution-Noncommercial-Share Alike 3.0 Unported license, as described at <http://creativecommons.org/licenses/by-nc-sa/3.0/>).

without IL-5 (Mishra et al., 1999; Kopf et al., 1996). Eotaxins (CCL11 and CCL24) are chemokines that recruit eosinophils, are central to eosinophil maintenance within the gastrointestinal tract, and can be up-regulated by IL-13 during allergic inflammation (Mishra et al., 1999; Rothenberg and Hogan, 2006; Voehringer et al., 2007). Eosinophils also use endothelial cell integrins, which can be increased by IL-4 and IL-13, to traffic into tissues (Blanchard and Rothenberg, 2009). The relative dependence of VAT eosinophils on these factors, including IL-4, IL-5, and IL-13, remains unknown.

Innate lymphoid type 2 cells (ILC2s) are recently characterized innate cells widely distributed in mammalian tissues (Spits and Di Santo, 2011). Also, designated innate helper type 2 cells (Price et al., 2010), nuocytes (Neill et al., 2010), or natural helper cells (Moro et al., 2010), ILC2s share features with other populations of innate lymphocytes, including NK cells (ILC1) and ILC3, comprising the ROR $\gamma$ T-dependent ILC: lymphoid tissue-inducer cells (LTic), innate IL-22 producing cells (also referred to as NK22, ILC22, NCR22, and NKR+ LTic) and innate IL-17-producing cells (Spits and Di Santo, 2011). ILCs all share a dependence on the transcription factor Id2 and the common- $\gamma$  chain ( $\gamma$ c) cytokine receptor (Spits and Di Santo, 2011). In response to the epithelial cytokines IL-25 and IL-33, ILC2s expand and produce large amounts of type 2 cytokines, particularly IL-13 and IL-5 (Hurst et al., 2002; Price et al., 2010; Moro et al., 2010; Neill et al., 2010), which can promote AAMs and eosinophils, respectively (Blanchard and Rothenberg, 2009; Martinez et al., 2009). Although ILC2s are functionally similar to CD4<sup>+</sup> T helper type 2 (Th2) cells (Price et al., 2010), ILC2s are widely distributed within tissues independent of antigenic stimulation and appear poised to respond to epithelial signals. One of the earliest descriptions of ILC2s identified them within lymphoid structures in mouse and human mesenteric adipose tissues (Moro et al., 2010). With this in mind, we sought to quantify ILC2s in metabolically active perigonadal VAT and determine whether these cells and the cytokines they produce, including IL-5 and IL-13, were responsible for the localization of eosinophils and AAMs to this tissue under basal conditions and after their activation by cytokines or in response to intestinal helminth infection.

## RESULTS

### Eosinophils and IL-5 promote insulin sensitivity and lean physiology

We previously reported metabolic consequences of eosinophil deficiency using *dblGata1* mice (Wu et al., 2011). Because IL-5 can promote local and systemic eosinophilia, we compared metabolic parameters in eosinophil-deficient and IL-5-deficient C57BL/6 mice during HFD challenge. We used Red5 mice, which contain a tandem-dimer red fluorescent protein (tdTomato) linked by an internal ribosomal entry site (IRES) to a Cre element, replacing the first exon of the *il5* gene (unpublished data), thus marking cells producing IL-5; Red5 homozygous mice are IL-5-deficient and the Cre element facilitates deletional studies based on IL-5 expression.

To control for potential genetic or microbiome contributions to these phenotypes, we compared IL-5-deficient Red5 homozygote and IL-5-sufficient Red5 heterozygote mice. Eosinophil-deficient and IL-5-deficient animals fed HFD for 18–20 wk gained more weight (Fig. 1 a), with increased total body adiposity (Fig. 1 b) and perigonadal VAT weight (Fig. 1 c), as compared with IL-5-sufficient mice. Fasting glucose levels were elevated in both strains of mice (Fig. 1 d), and both had impaired glucose (Fig. 1 e) and insulin tolerance (Fig. 1 f and unpublished data). These findings support and extend our previous results (Wu et al., 2011) to implicate IL-5 in metabolic homeostasis.

To further understand the mechanisms by which eosinophils and IL-5 influence metabolism, we placed eosinophil-deficient and -sufficient animals on HFD for 12 wk in metabolic cages. Although food and water intake and physical activity were not altered (unpublished data), total oxygen consumption (VO<sub>2</sub>) and energy utilization (heat) were decreased in eosinophil-deficient mice (Fig. 1, g and h); similar results occurred in IL-5-deficient animals (unpublished data). Thus, eosinophils and IL-5 do not alter caloric intake or caloric expenditures by enhancing physical activity. Instead, they may act in metabolically relevant tissue to promote increased oxidative metabolism and limit inflammation. Consistent with these findings, activation of iNKT IL-4 production (Lynch et al., 2012; Ji et al., 2012a) or exogenous IL-4 administration (Ricardo-Gonzalez et al., 2010) each promoted loss of adiposity and insulin sensitivity.

### ILC2s are the major source of IL-5 and IL-13 in VAT

ILC2s have been implicated in promoting eosinophil influx into tissues such as the lung and intestines during allergic inflammation (Neill et al., 2010; Price et al., 2010; Liang et al., 2012). We used flow cytometry to analyze perigonadal VAT to ascertain a potential role for ILC2s in controlling eosinophils in this tissue. Perigonadal adipose tissue was isolated and digested to yield the stromal vascular fraction (SVF) enriched for hematopoietic cells, endothelial cells, and other stromal components, but devoid of adipocytes. After using lineage markers to exclude B cells, T cells, and NK cells, we could readily identify a discrete population of lymphoid cells in the SVF-expressing receptors for IL-2 (CD25), IL-7, and IL-33 (Fig. 2, a and b), as well as intracellular Gata3 (Fig. 2 b). These markers were previously demonstrated for ILC2s (Moro et al., 2010; Neill et al., 2010; Price et al., 2010). Similar to other ILC2s, VAT ILC2s were present in Rag-deficient mice but absent in Rag x  $\gamma$ c-deficient and IL-7R $\alpha$ -deficient mice (Fig. 2, a–c), strains previously shown to lack ILC2s. VAT ILC2s were present in male and female mice and in C57BL/6 and BALB/c mice in both WT and Rag-deficient (T/B cell-deficient) backgrounds, although consistently more abundant in C57BL/6 mice (see also Fig. 4 d, bottom, and not depicted). Thus, the SVF of perigonadal adipose tissue contains innate lymphoid cells with the phenotype of previously described ILC2s (Moro et al., 2010; Neill et al., 2010; Price et al., 2010).

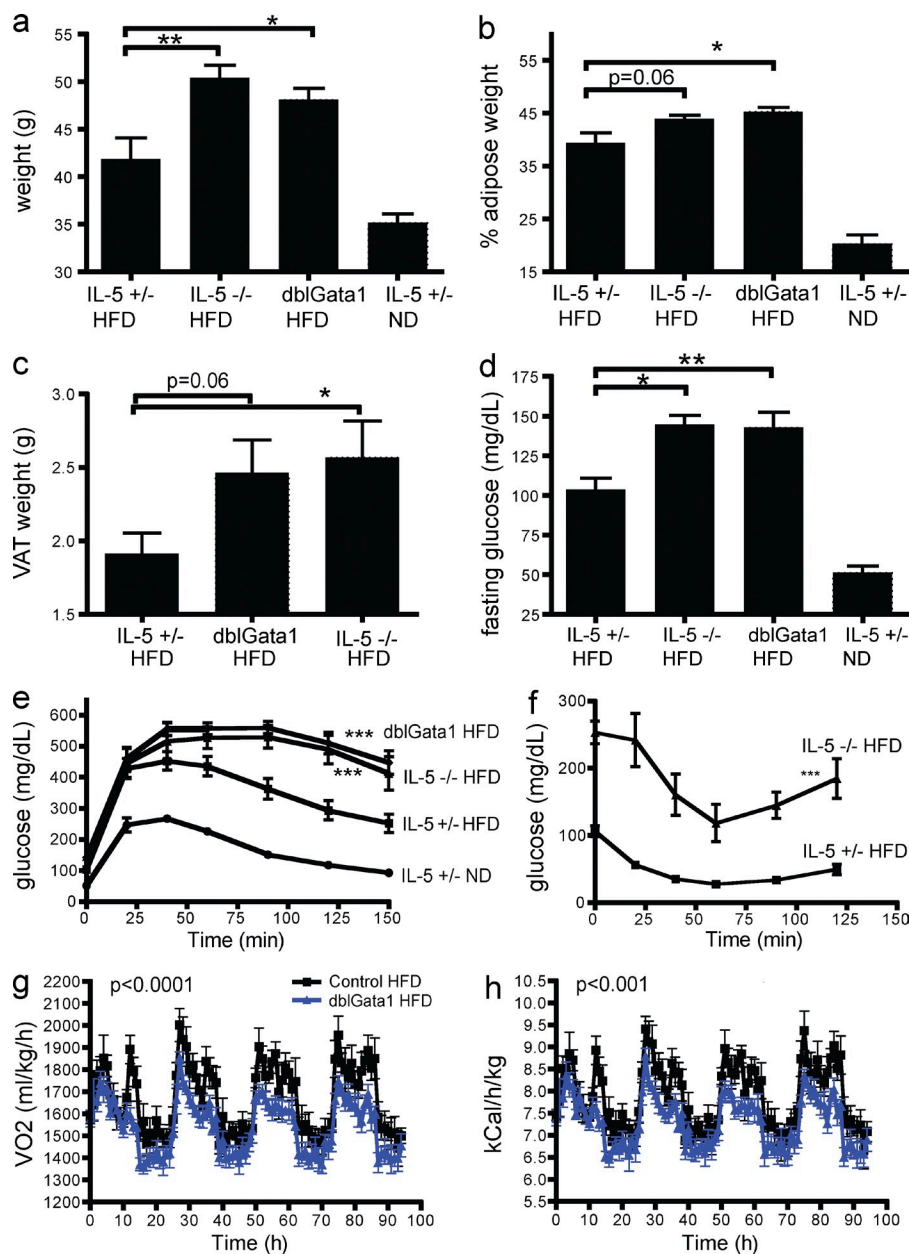


**Figure 1. Deficiency of IL-5 or eosinophils promotes obesity and insulin resistance and decreases oxidative respiration and heat production in mice on HFD.**

(a–c) Mice of the indicated genotype were fed HFD or ND for 18–20 wk, and then total weight (a), percent adiposity by EchoMRI (b), and terminal perigonadal VAT weight (c) were determined. Results are representative of three independent experiments and include four to six animals per cohort. Fasting blood glucose (d), glucose tolerance testing (e) and insulin tolerance testing (f) were performed in mice on ND or HFD for 18–20 wk. Results are representative of three experiments. IL-5<sup>+/-</sup>, Red5 C57BL/6 R<sup>+</sup> heterozygotes; IL-5<sup>-/-</sup>, Red5R/R homozygous IL-5 knockouts. (g and h) CLAMS analysis was performed using individually housed groups of six C57BL/6 or C57BL/6 *dbiGata1* eosinophil-deficient mice after maintenance on HFD for 12 wk. Variations in oxygen consumption (g) and energy expenditure over time (h) were pooled among animals in each group and statistical analysis was performed using pairwise comparisons. Error bars are the mean ± SEM. P-values are shown.

To assess the contribution of VAT ILC2s to the total IL-5 and IL-13 cytokine production in VAT, we used reporter mice with knock-in fluorescent alleles at various gene loci, thus allowing interrogation of the cytokine expression of these cells without the need for restimulation *ex vivo*. Both adipose SVF cells from Red5 mice, which mark IL-5-expressing cells with tdTomato expression, and YetCre13 × ROSA-YFP mice, which functionally mark cells that have ever expressed IL-13 by establishing constitutive YFP expression from the ROSA26 locus (Price et al., 2010), each contained cells marked by *in situ* IL-5 and IL-13 expression (Fig. 2 d). IL-5-expressing cells were negative for the myeloid marker CD11b, and included a small subset of CD4<sup>+</sup> CD3ε<sup>+</sup> IL33R<sup>+</sup> (T1/ST2<sup>+</sup>) Th2 cells (5–15%) and a large population of lineage-negative cells (85–95%). These VAT lineage-negative cells expressed

CD25 (IL2Rα), IL33R (T1/ST2), CD122 (IL2Rβ), Thy1.2 (CD90.2), c-Kit, Sca-1, and KRLG1, and were uniformly negative for T cell markers, including CD4, CD8, CD3ε, TCR-β, and TCR-γδ (Fig. 2 e), consistent with previously described ILC2s (Moro et al., 2010; Neill et al., 2010; Price et al., 2010). VAT B cells, CD8<sup>+</sup> T cells, CD3ε<sup>+</sup> CD4<sup>-</sup> CD8<sup>-</sup> “double-negative” T cells, macrophages, eosinophils, and α-galactosylceramide (αGC)-reactive invariant NKT cells (iNKT) did not show IL-5 fluorescence (Fig. 2 f and gating in Fig. S2), consistent with previous studies about lung IL-5<sup>+</sup> cells (Ikutani et al., 2012). Similar results were found for VAT IL-13-expressing cells, although small percentages of eosinophils (0.2–0.4%) and iNKT cells (3–5%) expressed IL-13 using lineage-tracked expression (Fig. 2 g). After prolonged IL-33 administration or helminth infection, ILC2s remain

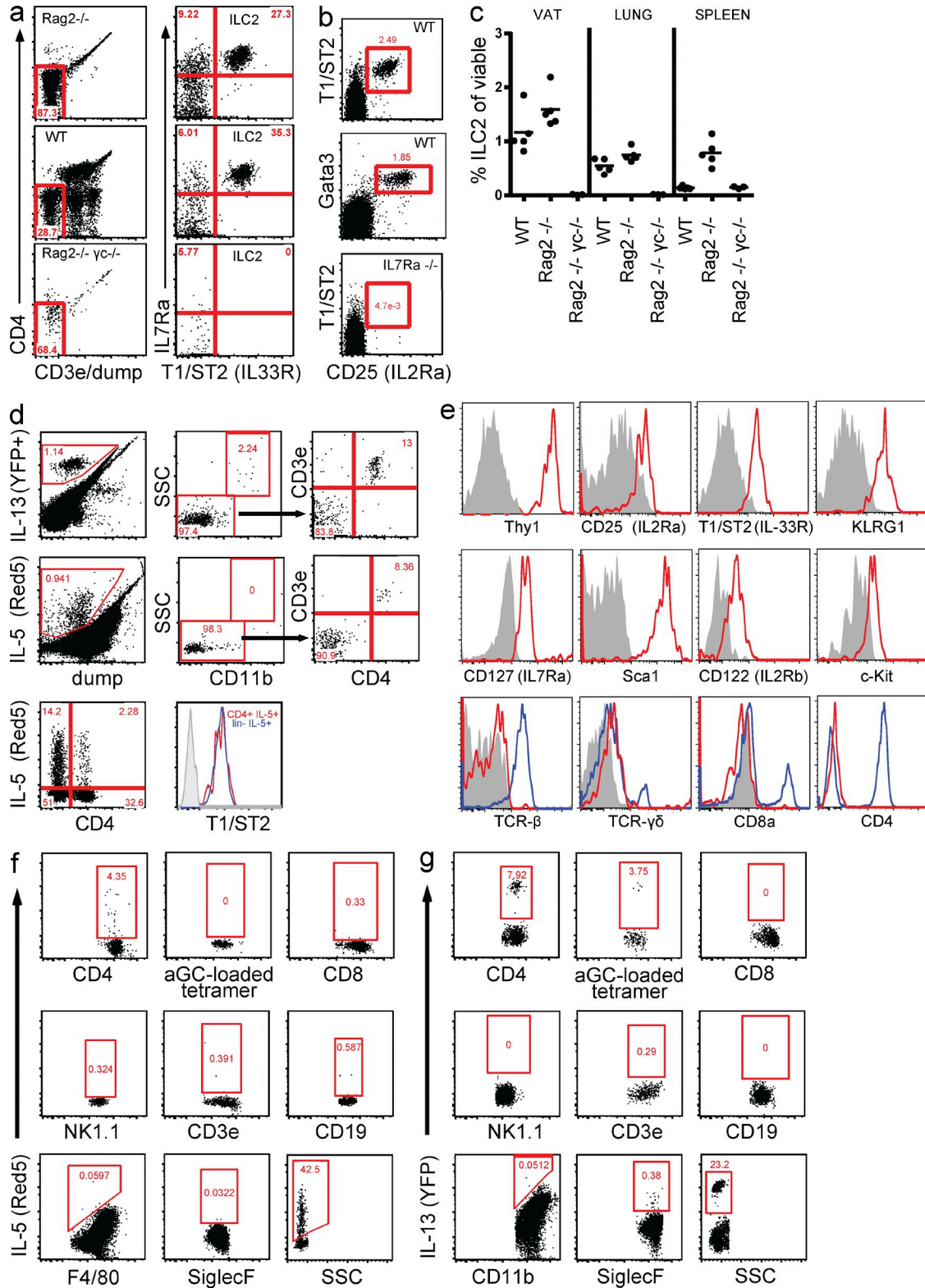


**Figure 2.** ILC2s are resident within VAT and are the primary cells expressing IL-5 and IL-13. (a and b) Representative ILC2s FACS plots (a and b) and frequency (c) of ILC2s from the VAT SVF of Rag2-deficient, WT, IL7Ra-deficient, and Rag2 $\times$   $\gamma_c$ -deficient C57BL/6 mice. Cells were pregated on lin<sup>-</sup> lymphoid cells (CD11b<sup>-</sup>, F4/80<sup>-</sup>, SiglecF<sup>-</sup>, SSC-lo, FSC-lo, CD45<sup>+</sup>; a) or lin<sup>-</sup> CD3e<sup>-</sup> CD4<sup>-</sup> (b). (d) Representative flow cytometry plots showing frequencies of IL-13<sup>+</sup> and IL-5<sup>+</sup> cells among various cell populations in VAT. (e) Expression of the indicated surface markers on VAT IL-5<sup>+</sup> lin<sup>-</sup> cells (ILC2, red line) compared with VAT CD3e<sup>+</sup> T cells (blue line) and isotype controls (gray; a–e) Data are representative of two or more experiments. (f and g) IL-5 and IL-13

the predominant IL-5<sup>-</sup> and IL-13<sup>-</sup>expressing cells, with no significant increased expression by macrophages, eosinophils, or other lymphocytes (Figs. S1 and S2 and unpublished data). Together, these results establish that ILC2s are the predominant IL-5<sup>-</sup> and IL-13<sup>-</sup>expressing cells in VAT and that rare Th2 cells account for most of the remaining cytokine-expressing cells.

As assessed using these reporter alleles, significant proportions of VAT ILC2s spontaneously produced IL-5 and IL-13 (Fig. 3, a and b), and this was particularly striking for IL-5. We could identify no phenotypic differences between cytokine-positive and -negative ILC2s, suggesting a uniform population with variable cytokine expression. IL-13 cytokine-marked cells, the great majority of which are ILC2s (Fig. 2 d), were readily detected in close apposition to the adipose vasculature and dispersed within VAT (Fig. 3c). Unlike ILC2s reported in mesenteric lymph nodes and mesenteric lymphoid clusters (Moro et al., 2010), we were unable to identify discrete lymphoid structures within perigonadal adipose tissue (unpublished data). In contrast to VAT ILC2s, bone marrow ILC2s (lineage<sup>-</sup> IL7R $\alpha$ <sup>+</sup> T1/ST2<sup>+</sup>; Brickshawana et al., 2011), which were also described as ILC2 precursors (Hoyler et al., 2012), did not express basal IL-13 as assessed with IL-13 lineage tracking ( $2.0 \pm 0.3\%$ ,  $n = 8$ ), although marrow ILC2s were predominantly IL-4 competent, as assessed using cells from 4get mice ( $85.5 \pm 7.4\%$ ,  $n = 3$ ). Although a subset of VAT ILC2s were competent to make IL-4 (4get<sup>+</sup>; Fig. 3, a and b), they were unmarked by reporter expression in KN2 mice (unpublished data), whose cells contain an IL-4 replacement allele and reveal cells actively producing IL-4 in situ (Mohrs et al., 2001; Wu et al., 2011), as previously described (Price et al., 2010; Wu et al., 2011).

To confirm the fidelity of the cytokine reporters and confirm additional cytokines secreted by these cells, VAT ILC2s (lineage-negative Thy1.2<sup>+</sup> CD25<sup>+</sup>) were purified by flow cytometry and placed in vitro for 72 h with various cytokines. Low amounts of IL-5, IL-6, IL-13, and GM-CSF spontaneously accumulated in the VAT ILC2 culture supernatants (Fig. 3, d and e, and unpublished data). After addition of IL-33, greater amounts of IL-5, IL-6, IL-9, IL-13, and GM-CSF accumulated (Fig. 3 d), and these cytokines increased further with the addition of IL-2 or IL-7, similar to results reported by ILC2s from other tissues (Moro et al., 2010; Halim et al., 2012). Together, these data suggest that VAT ILC2s spontaneously produce IL-5 and IL-13, and can respond to IL-33 with high levels of cytokine production, as shown for other ILC2s. Although rare in VAT, IL-5<sup>+</sup> (Red5<sup>+</sup>) CD4<sup>+</sup> T cells revealed a similar capacity to produce IL-2, IL-5, IL-6, IL-13, and GM-CSF after in vitro culture with PMA/ionomycin (Fig. 3 e). These data indicate IL-5<sup>+</sup> ILC2s are numerically predominant within VAT, but otherwise have a similar cytokine capacity to IL-5<sup>+</sup> Th2 cells.

### ILC2s are required to sustain adipose eosinophils and AAMs

Eosinophils home to and are sustained in VAT, where they promote AAM maintenance and systemic insulin sensitivity (Wu et al., 2011). As assessed after mitotic labeling during bone marrow differentiation, eosinophils had significantly lower turnover in VAT as compared with spleen and lung, consistent with the presence of recruitment, retention, or survival signals in adipose tissue (Fig. 4 a). Although present in Rag-deficient mice, VAT eosinophils were substantially and tissue-specifically reduced in Rag  $\times$   $\gamma_c$ -deficient mice that lack ILC2s (Fig. 4 b). Prolonged HFD results in a decline of VAT eosinophils, as previously described (Wu et al., 2011), which is associated with a loss of VAT ILC2s but increased numbers of total VAT macrophages and CD8<sup>+</sup> T cells (Fig. 4 c). In contrast, lung ILC2s were not reduced after HFD (unpublished data). Indeed, VAT ILC2 cell numbers correlate strongly with VAT eosinophils across multiple mouse WT strains, genetic mutations, and dietary perturbations, whereas total CD4<sup>+</sup> T cells show no corresponding correlation (Fig. 4 d).

To assess the effects of deleting IL-13-expressing ILC2s on adipose eosinophils, we crossed the YetCre13 mice to ROSA-DTA deleter mice, which led to diphtheria toxin A-mediated death of cells that express IL-13 (Voehringer et al., 2008). These IL-13 deleter mice had an  $\sim 40\%$  loss of adipose ILC2s, consistent with the IL-13 expression data (Fig. 4 e), and had a significant reduction in adipose tissue eosinophils that was not apparent in spleen or bone marrow (Fig. 4 f). Total VAT CD4<sup>+</sup> T cells and macrophages were not affected by deletion of IL-13-producing cells (Fig. 4 e), although rare IL-13<sup>+</sup> CD4<sup>+</sup> T cells were likely deleted. In contrast to the IL-13 deleter mice, deficiency of IL-4/IL-13 or STAT6 did not affect basal levels of VAT or spleen eosinophils (Fig. 4, d and g, unpublished data), indicating that although VAT ILC2s can produce IL-13, other ILC2-derived factors are required to sustain VAT eosinophils.

We performed similar studies using Red5 mice, which contain a disrupted *il5* gene replaced with a fluorescent td-Tomato with an embedded Cre recombinase. Eosinophils in adipose were strongly dependent on IL-5. Thus, Red5 heterozygous mice (IL-5<sup>+/-</sup>) had fewer adipose eosinophils than did mice with two intact *il5* alleles (WT), and IL-5-deficient Red5 homozygous mice (IL-5<sup>-/-</sup>) containing two marker alleles were drastically depleted of adipose eosinophils (Fig. 4 h). These effects of IL-5 deficiency were greater on adipose eosinophils compared with systemic eosinophils, with a 12–14-fold reduction in VAT (Fig. 4 h) versus a 2–3-fold reduction in spleen, blood, and small intestine (unpublished data). Although IL-5-deficient Red5 homozygous mice, similar to prior studies in eosinophil-deficient mice (Price et al., 2010), had normal numbers of ILC2s (unpublished data), Red5 mice containing a ROSA-DTA deleter allele exhibited significant depletion of total adipose ILC2s (Fig. 4 i), IL-5<sup>+</sup> (Red5<sup>+</sup>)

expression on the following VAT populations: CD4<sup>+</sup> T cells (CD4), iNKT (aGC-loaded tetramer), CD8<sup>+</sup> T cells (CD8), NK cells (NK1.1), CD3 $\epsilon$ <sup>+</sup> double-negative T cells (CD3 $\epsilon$ ), B cells (CD19), macrophages (CD11b), eosinophils (SiglecF), and lin<sup>-</sup> cells (SSC). Cells were pregated as shown in Fig. S2. Data are representative of two or more experiments.

ILC2s (Fig. 4 j), and almost complete ablation of adipose eosinophils (Fig. 4 h). Similar to IL-13 deleter animals, VAT from IL-5 deleter mice had normal numbers of macrophages, CD8<sup>+</sup> T cells, and total CD4<sup>+</sup> T cells. When assessed specifically for IL-5<sup>+</sup> CD4<sup>+</sup> T cells, IL-5 deleter animals also efficiently deleted the rare IL-5<sup>+</sup> Th2 cells (Fig. 4 j). However, as ILC2s are the predominant IL-5<sup>+</sup> VAT cell (85–95%), and VAT eosinophils are normal to elevated in T cell-deficient Rag animals (Fig. 4 b), we conclude that ILC2-expressing IL-5 are the primary cells required for the maintenance of visceral adipose eosinophils under basal conditions.

Adipose AAMs, like eosinophils, are present in the SVF of VATs in lean mice (Schipper et al., 2012). IL-13, like IL-4, can promote an AAM phenotype, which in mice can be revealed by expression of signature target genes such as arginase-1. We previously determined a role for eosinophils and hematopoietic IL-4/IL-13 in sustaining lean adipose AAMs, but

could not conclusively identify which cells produced these cytokines (Wu et al., 2011). We used YARG mice containing a fluorescent arginase-1 knock-in reporter allele to assess numbers of adipose AAMs, as previously described (Reese et al., 2007; Wu et al., 2011). As assessed by flow cytometry of dispersed SVF cells, adipose AAMs were depleted in  $\gamma_c$ -deficient mice (Fig. 4 k) and in IL-13 deleter mice (Fig. 4 l), strains that have absent or diminished ILC2s. Thus, adipose AAMs as assessed by arginase-1 expression are dependent on ILC2s, and loss of ILC2s based on their cytokine expression or dependence upon the  $\gamma_c$  cytokine chain results in a significant reduction in basal adipose AAMs.

**Exogenous IL-33 results in ILC2-dependent increases in adipose eosinophils and AAMs**

ILC2s were initially revealed by their capacity to release IL-13 and IL-5 in response to IL-25 and IL-33, epithelial cytokines

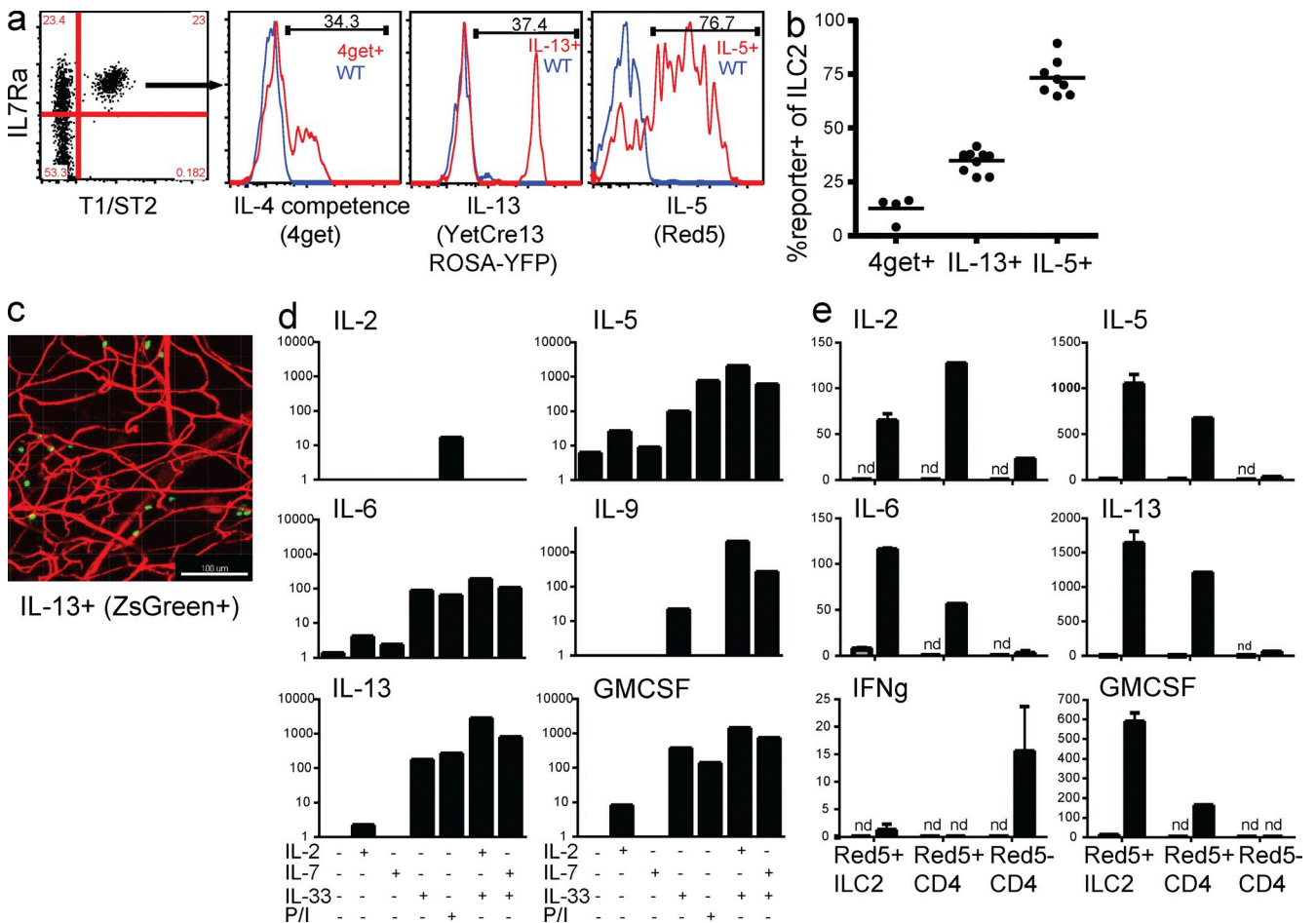


**Figure 3. VAT ILC2s spontaneously produce IL-5 and IL-13 in vivo and ex vivo, and respond robustly to IL-33.** Reporter cytokine expression by VAT ILC2s ( $lin^-$  IL7R $\alpha^+$  T1/ST2<sup>+</sup>) from 4get (IL-4 competence), Red5 (IL-5), and YetCre13 x ROSA-YFP (IL-13 reporter) mice (a), with percentages of VAT ILC2s positive for each cytokine marker (b) are shown. (c) Representative image shows spontaneous IL-13 reporter<sup>+</sup> cells (YetCre13 YFP x ROSA-ZsGreen) in freshly isolated, whole mounted VAT. (d) VAT total ILC2s ( $lin^-$  thyl.2<sup>+</sup> CD25<sup>+</sup>) were sorted and cultured in vitro for 72 h with the indicated combinations of IL-2, IL-7, IL-33, and PMA/ionomycin, and supernatant cytokine levels were determined (picogram per milliliter). (e) VAT IL-5<sup>+</sup> ILC2s ( $lin^-$  thyl.2<sup>+</sup> Red5<sup>+</sup>), IL-5<sup>+</sup> (Red5<sup>+</sup>) CD4<sup>+</sup> T cells, and IL-5-negative (Red5<sup>-</sup>) CD4<sup>+</sup> T cells were cultured with IL-7 (first bar) or PMA/ionomycin (second bar; d and e). Results are representative of two or more experiments. (a) Numbers in brackets or over lines indicate percentage of cells within the gate. Nd, not detected.

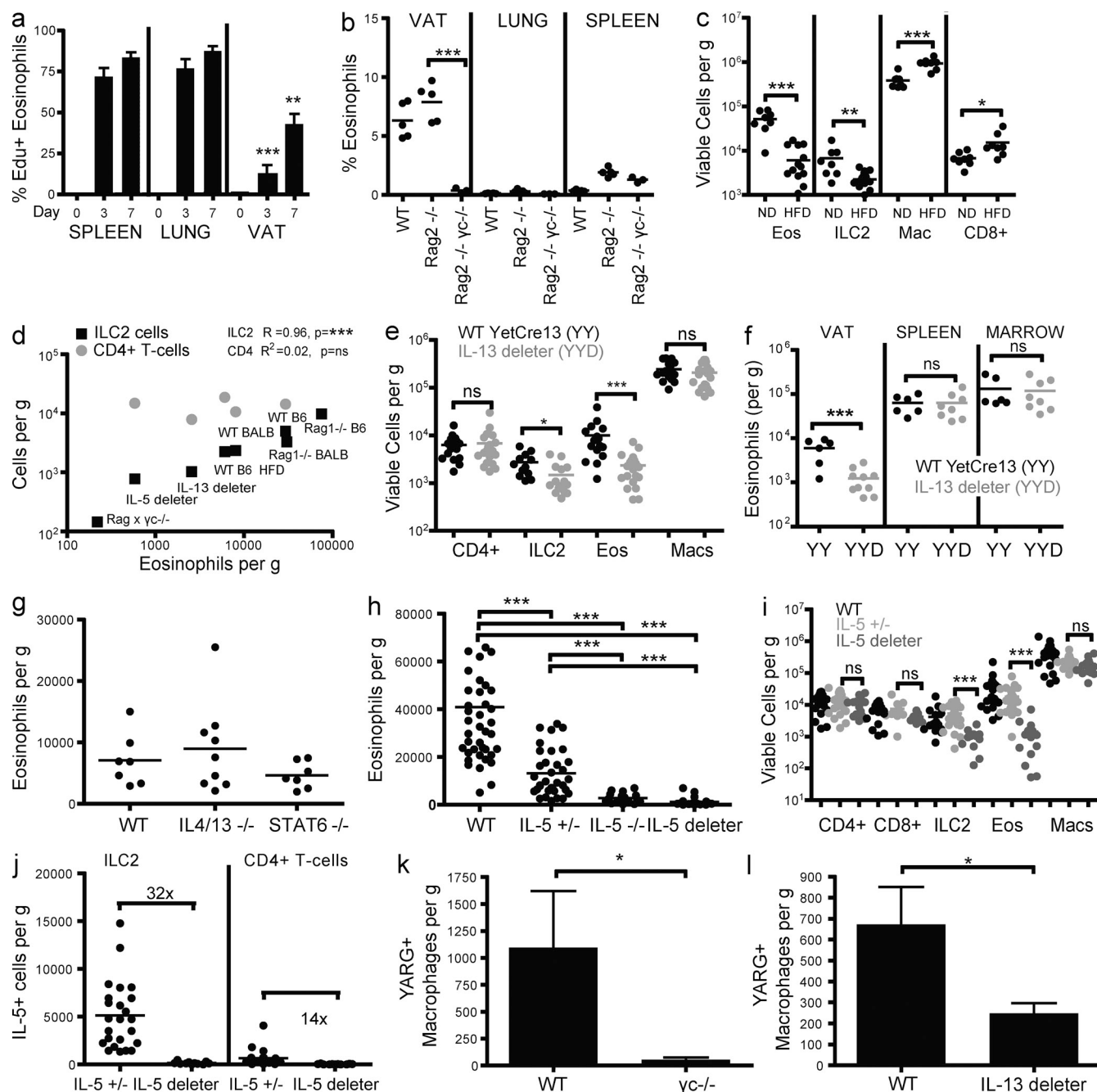


**Figure 4. VAT eosinophils and AAMs are dependent on ILC2s.** (a) C57BL/6 male mice were injected i.p. for the indicated number of days shown with 250  $\mu$ g Edu per mouse. FACS analysis was performed after pre-gating on eosinophils (Fig. S1). Data are from one experiment with three animals per group, and are representative of two independent experiments. (b) Frequency of eosinophils among total viable VAT, lung, or spleen cells from WT, Rag2-deficient, and Rag2 $\times$   $\gamma$ c-deficient C57BL/6 mice. Data are representative of three experiments. (c) WT C57BL/6 mice were fed a ND or HFD for 3–4 mo, and VAT SVF was examined for immune cell composition. Pooled data from three independent experiments are shown. (d) Correlation between VAT ILC2s or VAT CD4 $^{+}$  T cells and VAT eosinophils. Mouse strains shown include Rag  $\times$   $\gamma$ c (Rag2 deficient  $\times$   $\gamma$ c deficient), WT BALB (WT BALB/c), Rag1 $^{-/-}$  (Rag1 deficient), WT B6 HFD (WT C57BL/6 fed HFD for 3–4 mo), IL-13 deleter (YetCre13 Y/Y  $\times$  ROSA-DTA BALB/c), and IL-5 deleter (Red5 R/R  $\times$  ROSA-DTA C57BL/6). Strains were fed ND unless indicated. Each data point represents pooled data from at least five mice over multiple experiments. Pearson correlation coefficient is shown with significance. CD4 $^{+}$  T cell data are not shown for strains on the Rag-deficient background. (e–i) ILC2s, CD4 $^{+}$  T cells, CD8 $^{+}$  T cells, macrophages, and eosinophils were enumerated from the VAT (or indicated compartment) from the indicated strains and tissues on a BALB/c background (e–g) or C57BL/6 background (h and i). Data were pooled from two or more experiments. (j) VAT IL-5 $^{+}$  (Red5 $^{+}$ ) ILC2s or IL-5 $^{+}$  (Red5 $^{+}$ ) CD4 $^{+}$  T cells from the strains indicated. (k and l) Arginase-1 $^{+}$  (YFP $^{+}$ ) AAMs were enumerated from WT YARG or  $\gamma$ c-deficient YARG C57BL/6 basal VAT (k) or WT YARG or YetCre13  $\times$  ROSA-DTA YARG (IL-13 deleter) BALB/c (l) homeostatic VAT. Results contain pooled data from two or more experiments with 2–4 mice per experiment. \*,  $P < 0.05$ ; \*\*,  $P < 0.01$ ; \*\*\*,  $P < 0.001$ .

implicated in allergic immunity (Fort et al., 2001; Schmitz et al., 2005). IL-33 has been identified in VAT and exogenous IL-33 was shown to promote Th2-associated cytokines and to improve insulin sensitivity in obese mice (Miller et al., 2010). After administering IL-33, we noted the rapid accumulation of eosinophils in VAT that was accompanied by a decrease in eosinophils in spleen and bone marrow, which is consistent with a rapid redistribution of eosinophils from systemic compartments to VAT (Fig. 5 a). Several types of adipose SVF cells expressed T1/ST2, a nonredundant component of the IL-33 receptor, including ILC2s, a proportion of CD4<sup>+</sup> T cells and, at low levels, eosinophils; VAT macrophages and CD8 T cells did not express the receptor under these conditions (Fig. 5 b, unpublished data). VAT T1/ST2<sup>+</sup> CD4<sup>+</sup> T cells were primarily FoxP3<sup>+</sup> T reg cells with fewer FoxP3<sup>-</sup> Gata3<sup>-hi</sup> Th2 cells (unpublished data). In response to IL-33, ILC2s rapidly increased their side-scatter and surface CD25 levels, as described for lung ILC2s (Bartemes et al., 2012), and decreased their surface levels of IL-7R $\alpha$  (Fig. 5 d). To confirm that these parameters indicate ILC2 cell activation, we assessed the cytokine response of ILC2s in IL-13 and IL-5 reporter mice. In IL-13 lineage-tracker mice, where only a subset of ILC2s are IL-13 cytokine marked under basal conditions (Fig. 3, a and b), increased numbers of IL-13<sup>+</sup> (YFP<sup>+</sup>) ILC2s were readily detected after administering IL-33 (Fig. 5 d). In contrast, VAT CD4<sup>+</sup> T cells revealed minimal increases in IL-13<sup>+</sup> (YFP<sup>+</sup>) CD4<sup>+</sup> T cells (Fig. 5 c). IL-33 also caused increased fluorescence intensity in VAT ILC2s in IL-5 (Red5) reporter mice (Fig. 5 d). Together, these findings are consistent with direct activation of ILC2 effector function by IL-33. After three days of daily IL-33 administration, total VAT eosinophils and macrophages continued to accumulate, although ILC2 cell numbers did not significantly increase (Fig. 5 f). Cell populations in the spleen were not significantly affected during this timeframe (Fig. 5 e). With prolonged IL-33 administration, ILC2s accumulate within VAT and systemically, as previously described (Neill et al., 2010), accompanied by a systemic eosinophilia and macrophage accumulation (Fig. 5, g and h). Even after prolonged IL-33 administration, ILC2s remain the predominant IL-5<sup>+</sup> cells in VAT, and IL-5<sup>+</sup> (Red5<sup>+</sup>) CD4<sup>+</sup> T cells expand minimally (Fig. S2). In contrast, FoxP3<sup>+</sup> T reg cells accumulate both systemically, as described previously (Turnquist et al., 2011; Brunner et al., 2011), and within VAT (unpublished data). We conclude that IL-33 rapidly activates VAT ILC2s and promotes VAT eosinophils and AAM, and, over time, leads to additional local and systemic accumulations of ILC2s and T reg cells.

To assess the requirement for ILC2 cell activation in mediating the adipose cellular effects of exogenous IL-33, we administered IL-33 or control PBS to IL-5 and IL-13 control or deleter mice. Similar experiments were performed in control or deleter mice crossed onto the YARG arginase-1 background to assess requirements for ILC2s in the accumulation of adipose AAMs. Although control mice rapidly increased adipose eosinophils and AAMs in response to IL-33, this effect was abrogated after crossing onto strains deficient in ILC2s,

including the IL-13 deleter and IL-5 deleter (Fig. 6, a, b, e, and f), and in IL7R $\alpha$ -deficient mice (Fig. 6 g, unpublished data). In contrast, eosinophil accumulation is normal in response to IL-33 in Rag1-deficient animals that lack B and T cells (Fig. 6 c) or in IL-4/-13-deficient animals (Fig. 6 a). Similar to the percentage data (Fig. 6, a, b, and e-g), total adipose eosinophils and AAM also accumulate after IL-33 administration in an ILC2-dependent manner, although the increase is more robust in genetic strains on the C57BL/6 genetic background (unpublished data). We conclude that ILC2s are required for the IL-33-mediated increases in VAT eosinophils and AAM.

VAT Arginase1<sup>+</sup> AAMs are dependent on eosinophils and IL-4/-13 (Wu et al., 2011); however, the precise cellular sources of these cytokines are unclear. Loss of VAT ILC2s decreases VAT YARG<sup>+</sup> AAM (Fig. 4, k and l), but also leads to a loss of VAT eosinophils (Fig. 4, b, e, f, and i). Therefore, it remained unclear if ILC2s have the capacity to promote AAM accumulation independent of eosinophils. After IL-33 administration, YARG<sup>+</sup> AAM can accumulate in VAT independent of eosinophils as revealed in *dblGata1* mutant mice (Fig. 6g), demonstrating that exogenous IL-33 can induce IL-13 from VAT ILC2s sufficient to promote adipose AAM. Nonetheless, our understanding of the relative contributions of VAT eosinophils and ILC2-derived IL-13 to AAM maintenance under homeostatic conditions remains incomplete.

### Intestinal helminth infection drives ILC2-dependent increases in adipose eosinophils

We previously reported that infection of mice with *Nippostrongylus brasiliensis*, a 10-d self-limited migratory helminth infection, resulted in a prolonged elevation of visceral adipose eosinophils that correlated with improved metabolic homeostasis when mice were placed on HFD (Wu et al., 2011). To assess whether ILC2 activation, which accompanies *N. brasiliensis* infection (Liang et al., 2012; Neill et al., 2010), is required for VAT eosinophil accumulation, we infected IL-13 and IL-5 reporter mice. By 2 wk after infection, total numbers of VAT ILC2s were not increased, but IL-13- and IL-5-secreting ILC2s were increased, as assessed using reporter mice (Fig. 7, a and b). As compared with control mice, which developed robust accumulations of VAT eosinophils, IL-5 deleter (Fig. 7c) and IL-13 deleter mice (Fig. 7d) developed little eosinophilia. IL-13 cytokine-marked ILC2s remain the predominant IL-13-expressing cells, similar to basal conditions, although VAT IL-13 expressing Th2 cells are modestly increased (Fig. 7a). Rag1-deficient animals accumulate VAT eosinophils similarly to WT animals (Fig. 7e). Thus, as with IL-33 administration, helminth infection activates VAT ILC2s to produce IL-5 and IL-13, and loss of IL-5- and IL-13-producing cells, but not loss of T cells, results in a failure to accumulate VAT eosinophils.

### DISCUSSION

ILC2s have been increasingly implicated in host type 2 immune responses associated with asthma and intestinal helminth



infection in mice and humans (Brickshawana et al., 2011; Chang et al., 2011; Mjösberg et al., 2011; Moro et al., 2010; Neill et al., 2010; Price et al., 2010; Halim et al., 2012; Ikutani et al., 2012; Klein Wolterink et al., 2012; Liang et al., 2012; Klein Wolterink et al., 2012). These cells were first identified by their capacity to respond to the epithelial cytokines IL-25 and IL-33 through the production of large amounts of

IL-13 and IL-5 (Fort et al., 2001; Hurst et al., 2002; Schmitz et al., 2005). During helminth infection or allergen challenge, ILC2s constitute the major innate cell source of these cytokines, and loss of these cells can compromise the host type 2 immune response (Brickshawana et al., 2011; Chang et al., 2011; Mjösberg et al., 2011; Moro et al., 2010; Neill et al., 2010; Price et al., 2010; Halim et al., 2012; Ikutani et al., 2012;

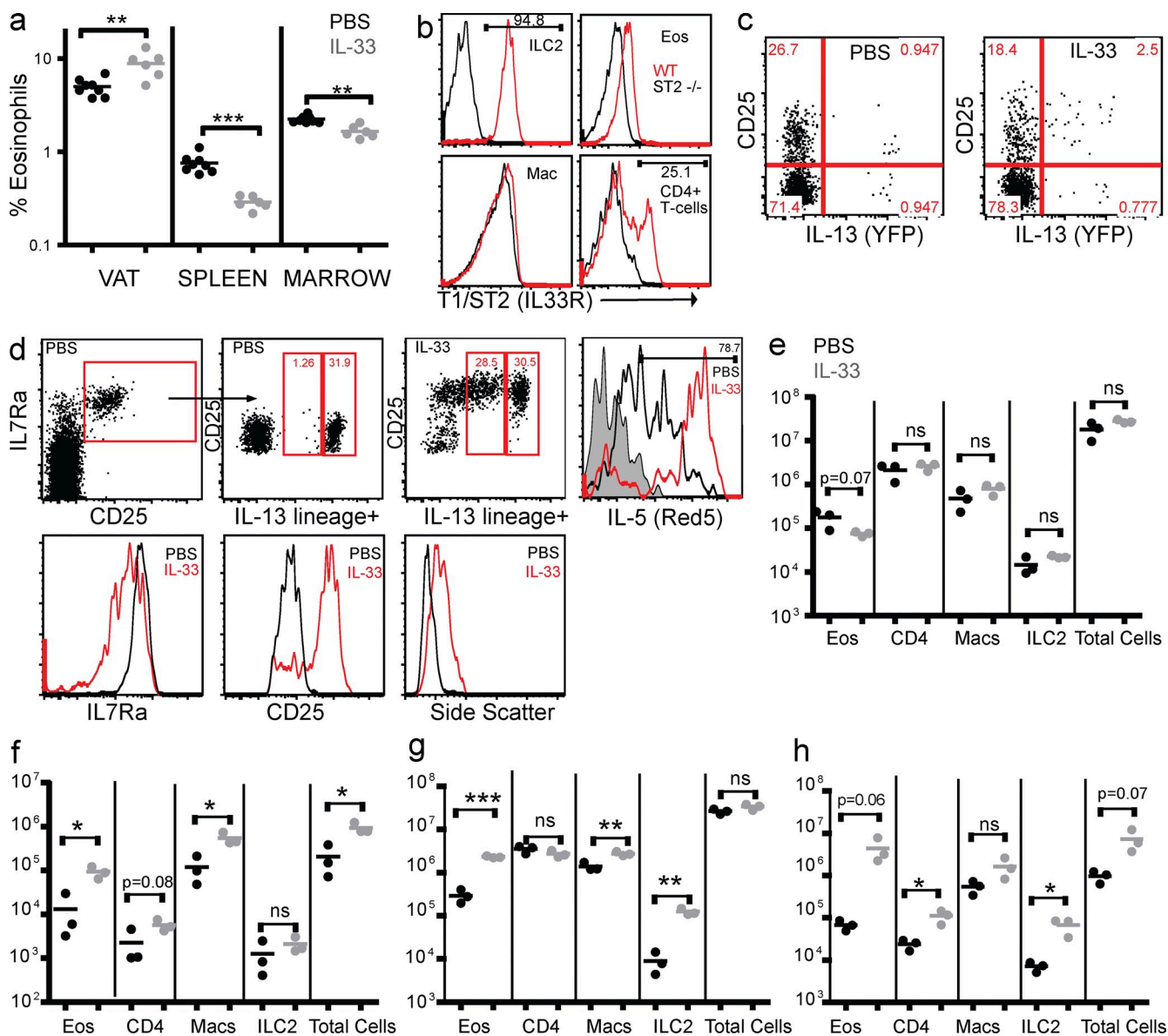


**Figure 5. IL-33 promotes ILC2 activation with IL-5 and IL-13 production and rapid VAT eosinophil accumulation.** (a) IL-33 (500 ng, gray circles) or PBS control (black circles) was administered i.p., and then, 12 h later, frequency of eosinophils was determined from VAT SVF, spleen, and bone marrow. Data are representative of three or more experiments. (b) Representative histograms of WT (red line) VAT ILC2s (lin<sup>-</sup> IL7Rα<sup>+</sup> CD25<sup>+</sup>), eosinophils (Eos), macrophages (Mac), and CD4<sup>+</sup> T cells (gating in Fig. S1), assessed for expression of T1/ST2 (IL-33R) and compared with T1/ST2-deficient (black lines) control animals (c and d) Representative FACS plots 24 h after IL-33 or PBS administration, pregated on CD4<sup>+</sup> T cells (c) or lin<sup>-</sup>, non-B cells, and non-T cells (d) in IL-13 lineage-tracking mice (YetCre13 Y<sup>+</sup> x Rosa-YFP) or IL-5 reporter mice (Red5 R<sup>+</sup> heterozygotes). Histograms in d are pregated on total lin<sup>-</sup> IL7Rα<sup>+</sup> CD25<sup>+</sup> VAT ILC2s. (e–h) IL-33 (500 ng, gray circles) or PBS (black circles) was administered daily for three consecutive days (e and f) or every other day for three doses (g and h), after which spleen (e and g) or VAT (f and h) eosinophils (Eos), CD4<sup>+</sup> T cells (CD4), macrophages (Macs), ILC2s (lin<sup>-</sup> IL7Rα<sup>+</sup> CD25<sup>+</sup>), and total cells were enumerated. Results are representative of two or more independent experiments. Numbers indicate percentages of cells within gates. \* , P < 0.05; \*\* , P < 0.01; \*\*\* , P < 0.001.

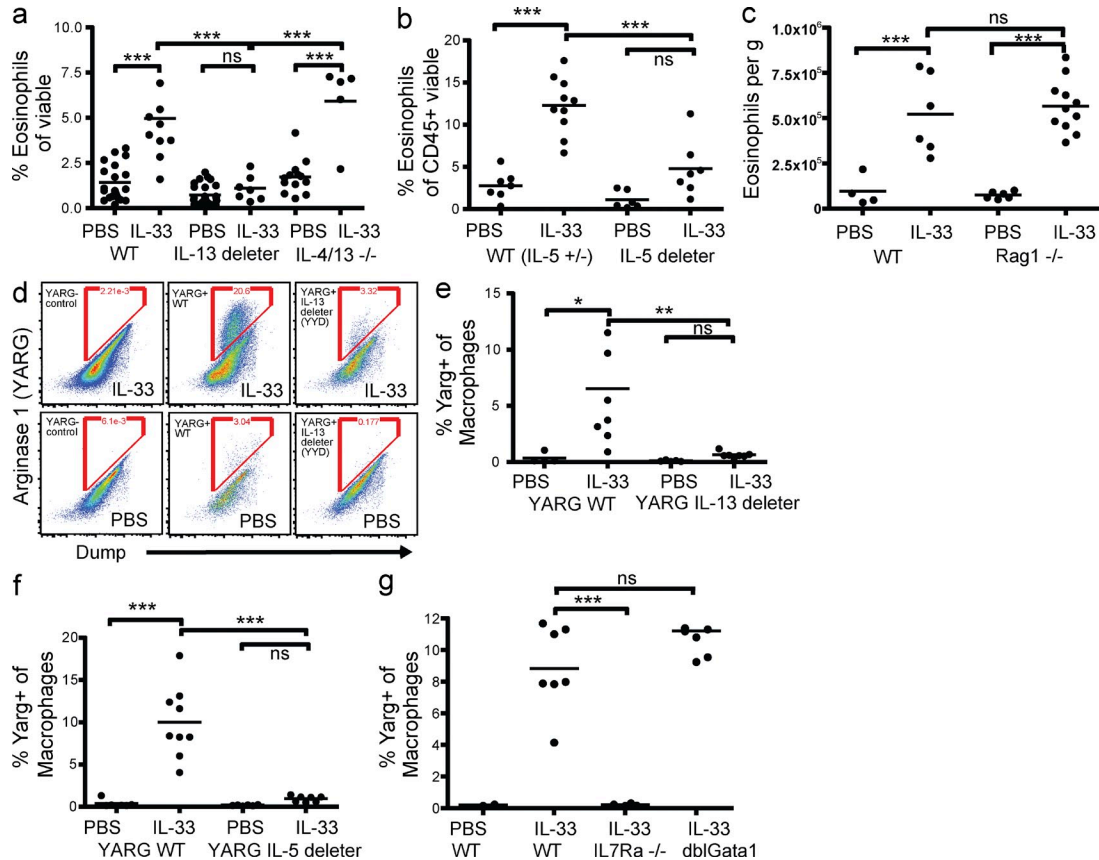


**Figure 6. IL-33 induces ILC2-dependent VAT accumulation of eosinophils and Arginase-1<sup>+</sup> AAMs.** (a–c) VAT eosinophils or VAT YARG<sup>+</sup> (YFP<sup>+</sup>) AAM (e–g) determined as a percentage of CD45<sup>+</sup> cells (a and b), total viable cells per g (c), or as a percentage of total macrophages (d–g) 24 h after administration of 500 ng IL-33 or PBS. (d) Representative FACS plots of YARG<sup>+</sup> AAM from the strains indicated, pregated on total macrophages (Fig. S1). IL-13 deleter mice, YetCre13 Y/Y x ROSA-DTA D/+ BALB/c; IL-5 deleter mice, Red5 R/+ x ROSA-DTA D/+ C57BL/6; mice with YARG reporter as noted (e–g). (a–c and e–g) Data were pooled from two or more experiments. Numbers indicate percentages of cells in gate. \*, P < 0.05; \*\*, P < 0.01; \*\*\*, P < 0.001.

Klein Wolterink et al., 2012; Liang et al., 2012). Despite subtle differences in surface markers used to characterize various laboratories' designation of these cells, their shared genetic and functional characteristics suggest a single cell type that is highly associated with allergic and antihelminth immunity. Recent studies have called attention to additional roles for ILC2-like cells in inflammatory processes (Monticelli et al., 2011; Chen et al., 2012), including limiting lung damage mediated by acute viral infection, potentially implicating ILC2s in reparative responses to tissue and organ injury. These studies did not find a role for IL-13 and IL-5, the canonical cytokines released in large abundance by ILC2s, in reestablishing organ homeostasis, leaving it unclear what the purpose of these cytokines might be in normal host physiology.

Using metabolic analysis, we demonstrate a role for IL-5 in sustaining metabolic homeostasis. As in eosinophil-deficient *dblGata1* animals, IL-5 deficiency promotes increased obesity and insulin resistance with HFD. We demonstrate that loss of IL-5 leads to a profound decrease in VAT eosinophils, with only modest alterations in systemic eosinophil pools, suggesting that a loss of VAT eosinophils is responsible for the metabolic consequences of IL-5 deficiency. However, we note that IL-5

deficiency is also associated with a partial loss of B1 B cells (Kopf et al., 1996), and these cells might also contribute to this phenotype. Loss of eosinophils or IL-5 does not affect animal food intake or physical exertion, but instead causes a decline in oxidative metabolism and energy expenditure (heat), ultimately resulting in increased adiposity and metabolic impairment. The precise molecular and cellular mechanisms leading to these metabolic alterations remain to be determined, but could reflect increased adipose inflammation secondary to the loss of adipose eosinophils and AAM. Whether eosinophils directly inhibit VAT inflammation or promote a lean state with decreased VAT mass that indirectly reduces inflammation remain intriguing questions. Using flow cytometric phenotyping, in situ imaging, and genetic approaches, we demonstrate that ILC2s are normal constituents of perigonadal VAT of the mouse. ILC2s reside in the SVF where eosinophils and AAMs are also present. Using cytokine reporter mice, we show that ILC2s are the primary producers of IL-5 and IL-13 under homeostatic conditions and, as demonstrated by functional deletion, that these cells are required for the constitutive localization of eosinophils and AAMs to VAT. Further, IL-33, shown to activate ILC2s systemically,

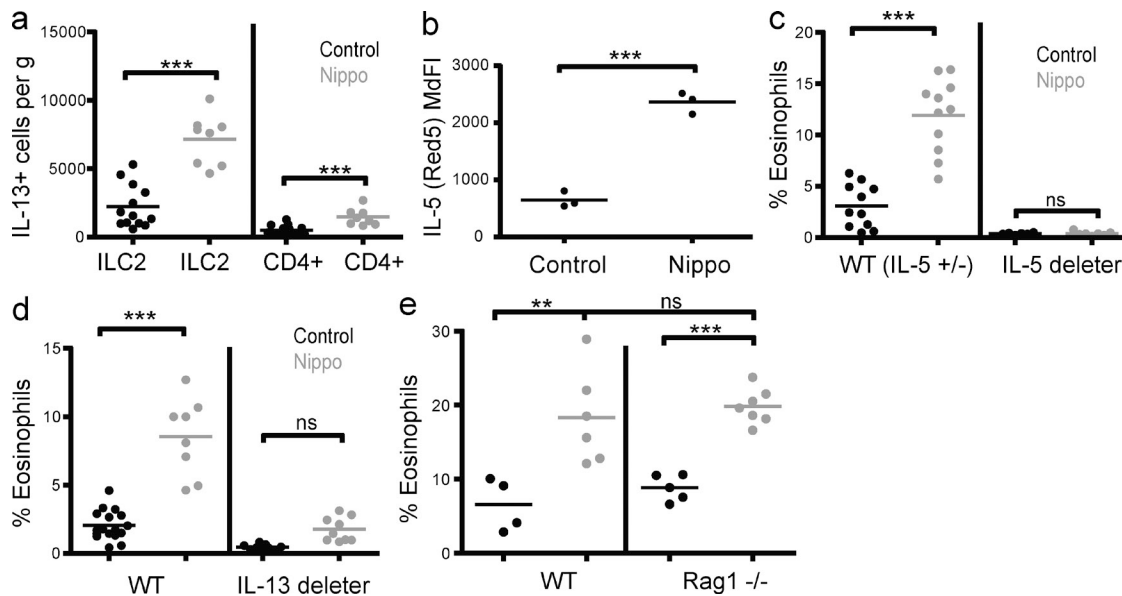


**Figure 7. *N. brasiliensis* infection promotes ILC2-dependent accumulation of VAT eosinophils.** (a–e) Mice were infected with *N. brasiliensis* and VAT was harvested ~2 wk post-infection (a–e) and analyzed by flow cytometry. (a) VAT IL-13 lineage-tracked ILC2s or IL-13<sup>+</sup> CD4<sup>+</sup> T cells (Yetcre13 Y<sup>+</sup> x ROSA-YFP) were enumerated. (b) IL-5<sup>+</sup> (Red5<sup>+</sup>) ILC2s were pregated and the median fluorescence intensity of Red5 (tdTomato) was determined. (c) VAT eosinophil frequency in IL-5<sup>+/-</sup> (Red5 R/+ heterozygotes) or IL-5 deleter (Red5 R/R x ROSA-DTA D/D) animals, (d) WT BALB/c or IL-13 deleter mice, or (e) WT C57BL/6 or Rag1-deficient C57BL/6 mice. Data were pooled from two to three experiments (a and c–e) or are representative of three experiments (b). \*, P < 0.05; \*\*, P < 0.01; \*\*\*, P < 0.001.

induces rapid increases in adipose eosinophils and AAMs that are dependent on ILC2s. Similarly, helminth infection promotes VAT eosinophilia that is dependent on ILC2s. In contrast, HFD results in a decline in VAT ILC2s that is associated with declining eosinophils. These data extend our understanding of these innate lymphoid cells, and, in conjunction with previous studies, suggest a mechanism by which metabolic needs of the organism might be regulated in response to chronic mucosal immune stimulation through activation of ILC2s.

Based on the capacity of epithelial cytokines to activate ILC2s, we administered IL-33 to mice and assessed the effects on adipose tissue. IL-33 rapidly activated ILC2s to increase expression of IL-5 and IL-13, and this led to the accumulation of eosinophils and AAMs in adipose tissue. As assessed by surface markers, side-scatter characteristics, and cytokine reporter expression, IL-33 directly activates adipose ILC2s. Deletion of these cells led to loss of eosinophil and AAM accumulation in adipose. IL-33 is abundant in adipose tissues where it may be produced and released by endothelial cells (Zeyda et al., 2012). Whether endothelial cells or other adipose cells undergo cell damage or can respond to environmental cues to release IL-33 remains unknown. Administration of IL-33 has beneficial metabolic effects in mice, consistent with those seen by increased eosinophils and AAMs (Miller et al., 2010), suggesting that IL-33-mediated ILC2 activation can promote insulin sensitivity.

Interestingly, IL-7 is necessary to sustain ILC2s and has also been localized to adipose (Lucas et al., 2012). TSLP is also present in adipose tissue (Turcot et al., 2012) and can sustain ILC2s in vitro (Halim et al., 2012). Further study is needed

to ascertain whether these or additional cytokines are necessary to sustain ILC2 homeostasis and activation in adipose tissues. Additionally, ILC2s have been reported to produce a variety of factors in addition to IL-5 and IL-13; we have confirmed that VAT ILC2s spontaneously produce IL-5, IL-6, IL-13, and GM-CSF protein in culture, and can be induced in vitro with exogenous IL-33 or PMA stimulation to produce these cytokines, as well as IL-2 and IL-9. The impact of each of these additional ILC2 cytokines on VAT cellular composition and metabolism requires further study.

VAT eosinophils are highly dependent on IL-5. Deletion of IL-5<sup>+</sup> cells or IL-13<sup>+</sup> cells, which are predominantly ILC2s, led to profound loss of VAT eosinophils and only minimally to eosinophils in other tissues. As such, the VAT eosinophil dependence upon IL-5 resembles many models of allergic and helminth-induced tissue eosinophilia, which can show strong IL-5 dependence (Foster et al., 1996; Kopf et al., 1996; Mould et al., 1997). However, ILC2s are widely distributed in tissues of unchallenged animals, and their presence alone is not associated with tissue eosinophils (Iktani et al., 2012; Price et al., 2010). VAT ILC2s may be relatively more abundant or activated than ILC2s from other tissues, sustaining VAT eosinophils and AAM. However, it is also likely that other VAT cells and signals contribute to the maintenance of these important cellular constituents. Indeed, VAT is an ample source of chemokines, including constitutive eotaxin-1 (Vasudevan et al., 2006), which could promote eosinophil trafficking into VAT. During helminth infections and allergic challenge in the lung, IL-5 promotes eosinophil production, survival, and retention, whereas IL-13 mediates eosinophil

recruitment through the promotion of tissue eotaxins (Blanchard and Rothenberg, 2009). In contrast, VAT eosinophils are present in the genetic absence of IL-13 or IL-13 signaling (STAT6), suggesting that constitutive factors, including eotaxins or other chemokines, may help recruit these cells. In addition, VAT eosinophil trafficking requires  $\alpha_L$ - and  $\alpha_4$ -mediated integrin signaling (Wu et al., 2011), indicating VAT endothelium contributes to eosinophil accumulation. Although VAT eosinophils are likely sustained by multiple pathways, ILC2s play an indispensable role under our experimental conditions.

Adipose AAMs and eosinophils are present in lean adipose, sustaining resistance of VATs to the proinflammatory effects of HFD and obesity (Chawla et al., 2011). Here, we demonstrate that ILC2 IL-5 is necessary to maintain VAT eosinophils, which are themselves required to sustain populations of Arginase-1<sup>+</sup> AAMs (Wu et al., 2011). ILC2s, in contrast to eosinophils (Fig. 2 f), produce ample IL-13 and could directly contribute to AAM polarization and maintenance. Indeed, with IL-33 stimulation ILC2s appear sufficient to promote Arginase-1<sup>+</sup> AAM, even in the absence of eosinophils. However, under basal conditions, eosinophils also promote AAM (Wu et al., 2011), suggesting ILC2 IL-13 may be insufficient to fully polarize and maintain VAT AAM under resting conditions. Consistent with this hypothesis, only a subset of ILC2s is marked for IL-13 expression, even using mice with lineage-tracked markers that reveal cells that have ever expressed IL-13 through their history. Ultimately, the relative contributions of eosinophils and ILC2 IL-13 production to AAM maintenance in lean adipose remain to be definitively elucidated.

The mechanisms by which eosinophils promote AAM remain poorly understood. Although IL-4 remains a candidate cytokine, only a small subset of adipose eosinophils (<1%) were marked for IL-4 protein expression as assessed using KN2 mice (Wu et al., 2011). Eosinophils produce abundant secreted products, including TGF $\beta$ , proteases, and RNase, which could also participate in AAM maintenance (Blanchard and Rothenberg, 2009). Adipocytes are also reported to be potential sources of IL-4 and IL-13 (Kang et al., 2008), but we have not observed fluorescence in adipocytes using IL-4 or IL-13 cytokine marker alleles (Wu et al., 2011; Fig. 3 c), and *il4* and *il13* transcripts are primarily found within the VAT SVF (Wu et al., 2011). VAT iNKT cells were recently proposed to mediate metabolic homeostasis and produce abundant IL-4 after TCR-stimulation that might promote AAM (Ji et al., 2012a; b; Lynch et al., 2012); in our mouse colony, iNKT cells are rare in VAT (Fig. S2). Finally, IL-5- and IL-13-expressing Th2 cells accumulate in VAT of older animals on normal diet (ND; unpublished data), and similar to VAT T reg cells (Feuerer et al., 2009), may provide an additional layer of adaptive regulation to maintain metabolic homeostasis. How these cells cooperate to promote AAM maintenance remains to be determined. Further, how AAMs themselves promote insulin sensitivity is also unclear, although proposed mechanisms include through the production of antiinflammatory cytokines and

insulin-sensitizing products, or through the activation of nonshivering thermogenesis (Nguyen et al., 2011; Chawla et al., 2011).

Intestinal helminth infections are widespread in feral animals, suggesting a long-standing mutualism. The host response is characterized by chronic type 2 immune responses, including the presence of epithelial mucus changes, Th2 cells, elevated IgE and mucosal mast cell hyperplasia, but also chronic eosinophilia and the accumulation of tissue AAMs. Similar responses, presumably dysregulated, accompany responses to ubiquitous environmental antigens in people with allergy and asthma. ILC2s respond to epithelial cytokines such as IL-25, IL-33, and TSLP, and have been implicated in both antihelminth and allergic immunity ((Brickshawana et al., 2011; Chang et al., 2011; Mjösberg et al., 2011; Moro et al., 2010; Neill et al., 2010; Price et al., 2010; Halim et al., 2012; Ikutani et al., 2012; Klein Wolterink et al., 2012; Liang et al., 2012). As shown here, adipose eosinophils, which accumulate after *N. brasiliensis* infection (Wu et al., 2011), do not accumulate in the absence of ILC2s, although accumulation is normal in T cell-deficient Rag mice. Of interest, both IL-33 administration and helminth infection promote insulin sensitivity in mice fed HFD (Miller et al., 2010; Wu et al., 2011), suggesting ILC2 activation and/or accumulation may be contributing to these metabolic effects. Based on prior studies, release of IL-25 and/or IL-33 during tissue-invasive helminth infection is likely (Moro et al., 2010; Neill et al., 2010), but further investigation will be necessary to show definitively which cytokines activate VAT ILC2s. The potential interactions between VAT ILC2s, Th2 cells and T reg cells, and their relative contributions to metabolic pathways during homeostasis and after helminth infection remain intriguing questions. Understanding the processes that sustain AAMs and eosinophils in VATs may offer new insights toward therapeutic strategies attempting to block the adverse effects of adipose inflammation and protect against insulin resistance and type 2 diabetes. Although further metabolic studies are needed, investigations of the role of these unusual innate lymphoid cells in adipose and other tissues are warranted, and may provide novel insights into more global aspects of vertebrate biology.

#### MATERIALS AND METHODS

**Mice.** Cytokine reporter mice previously described include 4get mice for tracking IL-4 competent cells (Mohrs et al., 2001; Wu et al., 2011), YetCre13 mice for tracking IL-13-producing cells (Price et al., 2010; Liang et al., 2012), and KN2 mice for tracking IL-4-producing cells (Mohrs et al., 2005; Wu et al., 2011). Where indicated, YetCre13 mice were crossed onto ROSA26-eYFP (The Jackson Laboratory) or ROSA26-ZsGreen (Ai6; The Jackson Laboratory; Madisen et al., 2010). The eYFP-Cre fusion protein downstream of the IL-13 locus in YetCre13 mice mediates deletion of the stop cassette from the ROSA26 locus, resulting in constitutive fluorophore expression in cells that have expressed IL-13. Newly generated Red5 mice contain a tdTomato-IRES-Cre replacement allele at the endogenous IL-5 start site, thus replacing the endogenous *il5* gene with tdTomato and revealing IL-5-expressing cells by red fluorescence. Homozygous Red5 mice (R/R) are IL-5 deficient, as both alleles are replaced by the marker construct, whereas heterozygous mice have one functional IL-5 copy (R/+). YARG mice contain a YFP marker

allele in the arginase-1 gene, permitting identification of AAMs, as previously described (Reese et al., 2007; Wu et al., 2011). ROSA-DTA mice contain a Cre-flanked flux-stop sequence upstream of diphtheria toxin  $\alpha$  (DTA) inserted into the constitutively expressed ROSA26 locus, thus causing Cre-expressing cells to be deleted, and have been previously described (Jackson; Voehringer et al., 2008). ROSA-DTA mice were crossed with YetCre13 or Red5 mice to create mice in which IL-13<sup>-</sup> or IL-5<sup>-</sup> expressing cells are deleted.

Additional mice used in these studies include Rag-deficient mice (Rag1; Jackson Laboratories; (Mombaerts et al., 1992) or Rag2 (Taconic Farms RAGN12), Rag2  $\times$   $\gamma_c$ -deficient mice (Taconic Farms 4111M), eosinophil-deficient  $\Delta$ dblGATA mice (Yu et al., 2002), IL-4/-13-deficient mice (McKenzie et al., 1999), Stat6-deficient mice (The Jackson Laboratory; Kaplan et al., 1996), IL7R $\alpha$ -deficient mice (The Jackson Laboratory; Peschon et al., 1994), and T1/ST2-deficient mice (Hoshino et al., 1999), and were crossed onto cytokine reporter alleles where designated. Mice used for these experiments were male animals fully backcrossed on C57BL/6 or BALB/c backgrounds, as designated. Mice were maintained in the University of California San Francisco specific pathogen-free animal facility, and all animal protocols were approved by and in accordance with the guidelines established by the Institutional Animal Care and Use Committee and Laboratory Animal Resource Center.

**Tissue preparation.** Perigonadal adipose tissue was used as representative VAT in all experiments. Testicles were removed and tissue was kept on ice in 0.5 ml of adipose digestion medium (low-glucose DMEM, 0.2 M Hepes, and 10 mg/ml fatty acid-poor BSA [Sigma]). VAT was finely minced with a multiple razor blades, dispersed by shaking into 10 ml of adipose digestion medium containing 0.2 mg/ml Liberase Tm (Roche) and 25  $\mu$ g/ml DNase I (Roche) at 37°C for 30–40 min with gentle agitation, and passed through 100- $\mu$ m filters to generate single-cell suspensions. Filters were washed with 10 ml FACS buffer (PBS, 3% FCS, 0.05% NaN<sub>3</sub>) and supernatants pooled. Cells were centrifuged at 1,000 *g* for 10 min and the cell pellets were resuspended in 5 ml FACS buffer, transferred to fresh tubes and centrifuged at 1,500 rpm for 5 min. The red blood cells were lysed using PharmLyse (BD) for 1 min, and the remaining cells were washed with FACS buffer, incubated with FcBlock, and stained with the indicated antibodies.

Spleen was prepared by mashing tissue through 70- $\mu$ m filters without tissue digestion, and processing similar to VAT. Bone marrow was prepared by carefully dissecting one femur and tibia, liberating hematopoietic cells with mortar and pestle into 10 ml FACS buffer, passing through a 70- $\mu$ m filter, and processing similar to VAT. Whole lung was prepared by harvesting both lung lobes into 5 ml DMEM media with 0.2 mg/ml Liberase Tm and 25  $\mu$ g/ml DNase 1, followed by tissue dissociation (GentleMacs; Miltenyi Biotec) using the “lung1 program,” followed by tissue digestion for 30 min at 37°C with gentle agitation. Samples were processed on the GentleMacs using the “lung2” program, passed through 70- $\mu$ m filters, and processed as described for VAT.

**Flow cytometry.** Monoclonal antibodies used for flow cytometry were as follows: allophycocyanin (APC)-eFluor 780-anti-CD4 (RM4-5; eBioscience); Qdot605-anti-CD4 (S3.5, Invitrogen); phycoerythrin (PE)-anti-Siglec-F (E50-2440; BD); APC- or Brilliant Violet 650- or Pacific Blue (PB)- anti-CD11b (M1/70; BioLegend); PE-Cy7- or PerCPCy5.5- anti-F4/80 (BM8; eBioscience); biotin-anti-pan-NK (CD49b; DX5; eBioscience), PB- anti-NK1.1 (PK136; BioLegend), biotin-anti-Fc $\epsilon$ R1 $\alpha$  (MAR-1; eBioscience); PB- or Alexa Fluor 488- or PerCPCy5.5- anti-CD3e (17A2; BioLegend); PB-anti-CD8 $\alpha$  (53-6.7; BioLegend); PerCPCy5.5-anti-CD19 (1D3; BD); PB-anti-CD19 (6D5; BioLegend), APC- or PE-anti-CD25 (IL2R $\alpha$ , PC61; BioLegend); PerCPCy5.5- or PE-Cy7-anti-CD127 (IL7R $\alpha$ , A7R34; eBioscience); Biotin-anti-T1/ST2 (DT8; MD Biosciences); APC- or APC-Cy7-anti-CD45 (30-F11; BioLegend). Secondary fluorophore for biotin-conjugated antibodies were eF605 (eBioscience), APC (BD), or FITC (BD). CD1d-aGC loaded and unloaded tetramer (PE or APC) were obtained from the National Institutes of Health tetramer facility. PE-Cy7 FoxP3 (FJK-16S; eBioscience) and A647 Gata3 (TWAJ; eBioscience) were used after first using a fixable live/dead stain (Invitrogen), and then fixing and permeabilizing cells per the

manufacturer's instructions. When used with fluorescent reporter strains, a brief 2-min “pre-fix” in 4% paraformaldehyde was performed before proceeding with eBioscience fix/perm instructions. Edu detection was achieved with the Click-it Edu A647 kit, after first staining for extracellular surface markers, per the manufacturer's instructions (Life Technologies).

Representative gating schemes for each population are shown in Fig. S1. ILC2s are identified as lineage negative (CD11b<sup>-</sup>, F4/80<sup>-</sup>, DX5<sup>-</sup>, CD3 $\epsilon$ <sup>-</sup>, CD4<sup>-</sup>, CD8 $\alpha$ <sup>-</sup>, CD19<sup>-</sup>, SiglecF<sup>-</sup>, Fc $\epsilon$ R1<sup>-</sup>, NK1.1<sup>-</sup>), FSC/SSC-low-to-moderate, CD45<sup>+</sup>, CD127 (IL7R $\alpha$ )<sup>+</sup> or thy1.2 (CD90.2)<sup>+</sup>, and T1/ST2 (IL33R)<sup>+</sup> or CD25 (IL2R $\alpha$ )<sup>+</sup> or KLRG1<sup>+</sup>, as indicated. CD4<sup>+</sup> T cells are identified as FSC/SSC-lo, CD45<sup>+</sup>, CD3 $\epsilon$ <sup>+</sup>, CD4<sup>+</sup>. CD8<sup>+</sup> T cells are identified as FSC/SSC-lo, CD45<sup>+</sup>, CD3 $\epsilon$ <sup>+</sup>, and CD8<sup>+</sup>. Eosinophils are identified as CD45<sup>+</sup>, side-scatter high, DAPI-lo, CD11b<sup>+</sup>, and SiglecF<sup>+</sup>. Adipose tissue macrophages are identified as CD45<sup>+</sup>, CD11b<sup>+</sup>, F4/80<sup>+</sup>, SiglecF-lo. All populations were routinely back-gated to verify purity and gating. Samples were analyzed on an LSR II (BD). For cell sorting, a FACS AriaII was used. Live lymphocytes were gated by DAPI exclusion, size, and granularity based on forward- and side-scatter. Data were analyzed using FlowJo software (Tree Star) and compiled using Prism (GraphPad Software). As indicated, VAT data were normalized per gram of adipose or as a percentage of total viable cells or percentage of CD45<sup>+</sup> hematopoietic cells, as indicated.

**Cell culture and cytokine analysis.** VAT from 8–15 WT C57BL/6 or Red5 (R/+ ) animals was pooled for cell sorting. Sorted ILC2s or CD4<sup>+</sup> T cells were transferred to 96-well plates in 100  $\mu$ l of eRMPi at 1,500 cells per well. Cytokines were added to culture media at 10 ng/ml, as indicated. PMA was used at 40 ng/ml and ionomycin was used at 500 ng/ml. Human IL-2 was used at 10 U/ml, and all other cytokines were purchased from R&D Systems. After 72 h of culture, supernatant cytokine levels were analyzed by cytokine bead arrays (BD) per the manufacturer's instructions.

**Metabolic assays and diet.** Male mice were fed normal chow diet (Mouse diet 20; PicoLab) and used between 8 and 15 wk of age, unless otherwise noted. Where indicated, C57BL/6 WT mice were fed HFD D12492 (60% kcal fat; Research Diets, Inc.) for 12–24 wk as noted. To measure animal adiposity and lean mass, MRI was performed using an EchoMRI 3-in-1 machine according to the manufacturer's instructions (Echo Medical Systems LTD). Glucose tolerance testing was performed after fasting mice overnight for 14 h and challenging with 1.5 g/kg glucose by i.p. injection. Fasting blood glucose was measured after a 4-h morning fast. Insulin tolerance tests were performed after a 4–5 h morning fast, injecting insulin i.p. (0.75 mU/g human insulin; Eli Lilly), and measuring blood glucose at the times indicated. Blood glucose was measured at indicated times using a glucometer (Bayer). Whole-animal metabolic analysis was performed using CLAMS cages (Comprehensive Laboratory Animals Monitoring System) per the manufacturer's instructions (Columbus Instruments). In brief, animals were singly housed and measurements were taken every 12 min for 4 d, including oxygen consumption, carbon dioxide output, food consumption, water consumption, and three unique measures of movement. Respiratory exchange ratio and heat were calculated as  $VCO_2/VO_2$  (RER) and  $VO_2(3.815 + 1.232 \times RER)$ ; heat, respectively. Heat,  $VO_2$ , and  $VCO_2$  were all normalized to effective body mass  $V_{xx} = V_{xx}/[(\text{weight(g)}/\text{mass unit})]^{0.75}$ , per the manufacturer's recommendations.

**Helminth infection and cytokine administration.** 500 third-stage larvae of *N. brasiliensis*, purified as described, were injected subcutaneously into mice (Voehringer et al., 2006). Mice were killed at the indicated time points and tissues were harvested and analyzed as previously described (Reese et al., 2007; Wu et al., 2011). IL-33 (R&D Systems) was given as 500 ng in 0.2 ml PBS i.p.

**Microscopy.** 5 min before sacrifice, animals were injected with 20  $\mu$ g CD31-APC (clone 390; eBioscience) to label vasculature. After VAT removal, the tissue was immediately mounted and examined by laser-scanning confocal microscopy (Nikon C1si). Images were resolved to 1.2  $\mu$ m/pixel in the x-y plane and 1.0  $\mu$ m in the z plane.

**Statistical analysis.** Unless otherwise noted, significance was determined by the Student's *t* test, with  $P < 0.05$  considered significant. \*,  $P < 0.05$ ; \*\*,  $P < 0.01$ ; \*\*\*,  $P < 0.001$ . Error bars represent standard error of the mean. Each data point represents one animal. When possible, data from multiple independent experiments were pooled, as indicated. In cases with multiple comparisons within an experiment ( $>2$ ), a one-tailed ANOVA was performed with Tukey's post-test correction.

We thank Drs. A. August, A. McKenzie, M. Steinhoff, and S. Wirtz for mice, A. DeFranco, C. Lowell and A. Ma for helpful comments on the manuscript, Zhi-En Wang for technical assistance, the Diabetes Endocrinology Research Core for assistance with CLAMS analysis, and N. Flores and M. Consengco for animal support.

This work was supported by AIO26918, AIO30663, AIO78869, HL107202, and P30 DK063720 from the National Institutes of Health, the UCSF Diabetes Family Fund (ABM), the Department of Laboratory Medicine discretionary fund (ABM), the Larry Hillblom Foundation, the Sandler Asthma Basic Research Center at UCSF and the Howard Hughes Medical Institute.

The authors have no conflicting financial interests.

Submitted: 30 August 2012

Accepted: 30 January 2013

## REFERENCES

- Bartemes, K.R., K. Iijima, T. Kobayashi, G.M. Kephart, A.N. McKenzie, and H. Kita. 2012. IL-33-responsive lineage- CD25+ CD44(hi) lymphoid cells mediate innate type 2 immunity and allergic inflammation in the lungs. *J. Immunol.* 188:1503–1513. <http://dx.doi.org/10.4049/jimmunol.1102832>
- Blanchard, C., and M.E. Rothenberg. 2009. Biology of the eosinophil. *Adv Immunol.* 101:81–121. [http://dx.doi.org/10.1016/S0065-2776\(08\)01003-1](http://dx.doi.org/10.1016/S0065-2776(08)01003-1)
- Brickshawana, A., V.S. Shapiro, H. Kita, and L.R. Pease. 2011. Lineage (-)Sca1+c-Kit(-)CD25+ cells are IL-33-responsive type 2 innate cells in the mouse bone marrow. *J. Immunol.* 187:5795–5804. <http://dx.doi.org/10.4049/jimmunol.1102242>
- Brunner, S.M., G. Schiechl, W. Falk, H.J. Schlitt, E.K. Geissler, and S. Fichtner-Feigl. 2011. Interleukin-33 prolongs allograft survival during chronic cardiac rejection. *Transpl. Int.* 24:1027–1039. <http://dx.doi.org/10.1111/j.1432-2277.2011.01306.x>
- Chang, Y.-J., H.Y. Kim, L.A. Albacker, N. Baumgarth, A.N.J. McKenzie, D.E. Smith, R.H. Dekruyff, and D.T. Umetsu. 2011. Innate lymphoid cells mediate influenza-induced airway hyper-reactivity independently of adaptive immunity. *Nat. Immunol.* 12:631–638. <http://dx.doi.org/10.1038/ni.2045>
- Chawla, A., K.D. Nguyen, and Y.P.S. Goh. 2011. Macrophage-mediated inflammation in metabolic disease. *Nat. Rev. Immunol.* 11:738–749. <http://dx.doi.org/10.1038/nri3071>
- Chen, F., Z. Liu, W. Wu, C. Rozo, S. Bowdridge, A. Millman, N. Van Rooijen, J.F. Urban Jr., T.A. Wynn, and W.C. Gause. 2012. An essential role for TH2-type responses in limiting acute tissue damage during experimental helminth infection. *Nat. Med.* 18:260–266. <http://dx.doi.org/10.1038/nm.2628>
- Feuerer, M., L. Herrero, D. Cipolletta, A. Naaz, J. Wong, A. Nayer, J. Lee, A.B. Goldfine, C. Benoist, S. Shoelson, and D. Mathis. 2009. Lean, but not obese, fat is enriched for a unique population of regulatory T cells that affect metabolic parameters. *Nat. Med.* 15:930–939. <http://dx.doi.org/10.1038/nm.2002>
- Fort, M.M., J. Cheung, D. Yen, J. Li, S.M. Zurawski, S. Lo, S. Menon, T. Clifford, B. Hunte, R. Lesley, et al. 2001. IL-25 induces IL-4, IL-5, and IL-13 and Th2-associated pathologies in vivo. *Immunity.* 15:985–995. [http://dx.doi.org/10.1016/S1074-7613\(01\)00243-6](http://dx.doi.org/10.1016/S1074-7613(01)00243-6)
- Foster, P.S., S.P. Hogan, A.J. Ramsay, K.I. Matthaei, and I.G. Young. 1996. Interleukin 5 deficiency abolishes eosinophilia, airways hyperreactivity, and lung damage in a mouse asthma model. *J. Exp. Med.* 183:195–201. <http://dx.doi.org/10.1084/jem.183.1.195>
- Halim, T.Y.F., R.H. Krauss, A.C. Sun, and F. Takei. 2012. Lung natural helper cells are a critical source of Th2 cell-type cytokines in protease allergen-induced airway inflammation. *Immunity.* 36:451–463. <http://dx.doi.org/10.1016/j.immuni.2011.12.020>
- Hoshino, K., S. Kashiwamura, K. Kuribayashi, T. Kodama, T. Tsujimura, K. Nakanishi, T. Matsuyama, K. Takeda, and S. Akira. 1999. The absence of interleukin 1 receptor-related T1/ST2 does not affect T helper cell type 2 development and its effector function. *J. Exp. Med.* 190:1541–1548. <http://dx.doi.org/10.1084/jem.190.10.1541>
- Hoyler, T., C.S.N. Klose, A. Souabni, A. Turqueti-Neves, D. Pfeifer, E.L. Rawlins, D. Voehringer, M. Busslinger, and A. Diefenbach. 2012. The transcription factor GATA-3 controls cell fate and maintenance of type 2 innate lymphoid cells. *Immunity.* 37:634–648. <http://dx.doi.org/10.1016/j.immuni.2012.06.020>
- Hurst, S.D., T. Muchamuel, D.M. Gorman, J.M. Gilbert, T. Clifford, S. Kwan, S. Menon, B. Seymour, C. Jackson, T.T. Kung, et al. 2002. New IL-17 family members promote Th1 or Th2 responses in the lung: in vivo function of the novel cytokine IL-25. *J. Immunol.* 169:443–453.
- Ikutani, M., T. Yanagibashi, M. Ogasawara, K. Tsuneyama, S. Yamamoto, Y. Hattori, T. Kouro, A. Itakura, Y. Nagai, S. Takaki, and K. Takatsu. 2012. Identification of innate IL-5-producing cells and their role in lung eosinophil regulation and antitumor immunity. *J. Immunol.* 188:703–713. <http://dx.doi.org/10.4049/jimmunol.1101270>
- Ji, Y., S. Sun, A. Xu, P. Bhargava, L. Yang, K.S.L. Lam, B. Gao, C.-H. Lee, S. Kersten, and L. Qi. 2012a. Activation of natural killer T cells promotes M2 Macrophage polarization in adipose tissue and improves systemic glucose tolerance via interleukin-4 (IL-4)/STAT6 protein signaling axis in obesity. *J. Biol. Chem.* 287:13561–13571. <http://dx.doi.org/10.1074/jbc.M112.350066>
- Ji, Y., S. Sun, S. Xia, L. Yang, X. Li, and L. Qi. 2012b. Short term high fat diet challenge promotes alternative macrophage polarization in adipose tissue via natural killer T cells and interleukin-4. *J. Biol. Chem.* 287:24378–24386. <http://dx.doi.org/10.1074/jbc.M112.371807>
- Kang, K., S.M. Reilly, V. Karabacak, M.R. Gangl, K. Fitzgerald, B. Hatano, and C.-H. Lee. 2008. Adipocyte-derived Th2 cytokines and myeloid PPARdelta regulate macrophage polarization and insulin sensitivity. *Cell Metab.* 7:485–495. <http://dx.doi.org/10.1016/j.cmet.2008.04.002>
- Kaplan, M.H., U. Schindler, S.T. Smiley, and M.J. Grusby. 1996. Stat6 is required for mediating responses to IL-4 and for development of Th2 cells. *Immunity.* 4:313–319. [http://dx.doi.org/10.1016/S1074-7613\(00\)80439-2](http://dx.doi.org/10.1016/S1074-7613(00)80439-2)
- Klein Wolterink, R.G., A. Kleinjan, M. van Nimwegen, I. Bergen, M. de Bruijn, Y. Levani, and R.W. Hendriks. 2012. Pulmonary innate lymphoid cells are major producers of IL-5 and IL-13 in murine models of allergic asthma. *Eur. J. Immunol.* 42:1106–1116. <http://dx.doi.org/10.1002/eji.201142018>
- Kopf, M., F. Brombacher, P.D. Hodgkin, A.J. Ramsay, E.A. Milbourne, W.J. Dai, K.S. Ovington, C.A. Behm, G. Köhler, I.G. Young, and K.I. Matthaei. 1996. IL-5-deficient mice have a developmental defect in CD5+ B-1 cells and lack eosinophilia but have normal antibody and cytotoxic T cell responses. *Immunity.* 4:15–24. [http://dx.doi.org/10.1016/S1074-7613\(00\)80294-0](http://dx.doi.org/10.1016/S1074-7613(00)80294-0)
- Liang, H.-E., R.L. Reinhardt, J.K. Bando, B.M. Sullivan, I.-C. Ho, and R.M. Locksley. 2012. Divergent expression patterns of IL-4 and IL-13 define unique functions in allergic immunity. *Nat. Immunol.* 13:58–66. <http://dx.doi.org/10.1038/ni.2182>
- Lucas, S., S. Taront, C. Magnan, L. Fauconnier, M. Delacore, L. Macia, A. Delanoye, C. Verwaerde, C. Spriet, P. Saule, et al. 2012. Interleukin-7 regulates adipose tissue mass and insulin sensitivity in high-fat diet-fed mice through lymphocyte-dependent and independent mechanisms. *PLoS ONE.* 7:e40351. <http://dx.doi.org/10.1371/journal.pone.0040351>
- Lynch, L., M. Nowak, B. Varghese, J. Clark, A.E. Hogan, V. Toxavidis, S.P. Balk, D. O'Shea, C. O'Farrelly, and M.A. Exley. 2012. Adipose tissue invariant NKT cells protect against diet-induced obesity and metabolic disorder through regulatory cytokine production. *Immunity.* 37:574–587. <http://dx.doi.org/10.1016/j.immuni.2012.06.016>
- Madisen, L., T.A. Zwingman, S.M. Sunkin, S.W. Oh, H.A. Zariwala, H. Gu, L.L. Ng, R.D. Palmiter, M.J. Hawrylycz, A.R. Jones, et al. 2010. A robust and high-throughput Cre reporting and characterization system

- for the whole mouse brain. *Nat. Neurosci.* 13:133–140. <http://dx.doi.org/10.1038/nn.2467>
- Martinez, F.O., L. Helming, and S. Gordon. 2009. Alternative activation of macrophages: an immunologic functional perspective. *Annu. Rev. Immunol.* 27:451–483. <http://dx.doi.org/10.1146/annurev.immunol.021908.132532>
- McKenzie, G.J., P.G. Fallon, C.L. Emson, R.K. Grencis, and A.N. McKenzie. 1999. Simultaneous disruption of interleukin (IL)-4 and IL-13 defines individual roles in T helper cell type 2-mediated responses. *J. Exp. Med.* 189:1565–1572. <http://dx.doi.org/10.1084/jem.189.10.1565>
- Miller, A.M., D.L. Asquith, A.J. Hueber, L.A. Anderson, W.M. Holmes, A.N. McKenzie, D. Xu, N. Sattar, I.B. McInnes, and F.Y. Liew. 2010. Interleukin-33 induces protective effects in adipose tissue inflammation during obesity in mice. *Circ. Res.* 107:650–658. <http://dx.doi.org/10.1161/CIRCRESAHA.110.218867>
- Mishra, A., S.P. Hogan, J.J. Lee, P.S. Foster, and M.E. Rothenberg. 1999. Fundamental signals that regulate eosinophil homing to the gastrointestinal tract. *J. Clin. Invest.* 103:1719–1727. <http://dx.doi.org/10.1172/JCI6560>
- Mjösberg, J.M., S. Trifari, N.K. Crellin, C.P. Peters, C.M. van Drunen, B. Piet, W.J. Fokkens, T. Cupedo, and H. Spits. 2011. Human IL-25- and IL-33-responsive type 2 innate lymphoid cells are defined by expression of CRTH2 and CD161. *Nat. Immunol.* 12:1055–1062. <http://dx.doi.org/10.1038/ni.2104>
- Mohrs, M., K. Shinkai, K. Mohrs, and R.M. Locksley. 2001. Analysis of type 2 immunity in vivo with a bicistronic IL-4 reporter. *Immunity.* 15:303–311. [http://dx.doi.org/10.1016/S1074-7613\(01\)00186-8](http://dx.doi.org/10.1016/S1074-7613(01)00186-8)
- Mohrs, K., A.E. Wakil, N. Killeen, R.M. Locksley, and M. Mohrs. 2005. A two-step process for cytokine production revealed by IL-4 dual-reporter mice. *Immunity.* 23:419–429. <http://dx.doi.org/10.1016/j.immuni.2005.09.006>
- Mombaerts, P., J. Iacomini, R.S. Johnson, K. Herrup, S. Tonegawa, and V.E. Papaioannou. 1992. RAG-1-deficient mice have no mature B and T lymphocytes. *Cell.* 68:869–877. [http://dx.doi.org/10.1016/0092-8674\(92\)90030-G](http://dx.doi.org/10.1016/0092-8674(92)90030-G)
- Monticelli, L.A., G.F. Sonnenberg, M.C. Abt, T. Alenghat, C.G.K. Ziegler, T.A. Doering, J.M. Angelosanto, B.J. Laidlaw, C.Y. Yang, T. Sathaliyawala, et al. 2011. Innate lymphoid cells promote lung-tissue homeostasis after infection with influenza virus. *Nat. Immunol.* 12:1045–1054. <http://dx.doi.org/10.1038/ni.2131>
- Moro, K., T. Yamada, M. Tanabe, T. Takeuchi, T. Ikawa, H. Kawamoto, J.-I. Furusawa, M. Ohtani, H. Fujii, and S. Koyasu. 2010. Innate production of T(H)2 cytokines by adipose tissue-associated c-Kit(+)Sca-1(+) lymphoid cells. *Nature.* 463:540–544. <http://dx.doi.org/10.1038/nature08636>
- Mould, A.W., K.I. Matthaei, I.G. Young, and P.S. Foster. 1997. Relationship between interleukin-5 and eotaxin in regulating blood and tissue eosinophilia in mice. *J. Clin. Invest.* 99:1064–1071. <http://dx.doi.org/10.1172/JCI119234>
- Neill, D.R., S.H. Wong, A. Bellosi, R.J. Flynn, M. Daly, T.K.A. Langford, C. Bucks, C.M. Kane, P.G. Fallon, R. Pannell, et al. 2010. Nuocytes represent a new innate effector leukocyte that mediates type-2 immunity. *Nature.* 464:1367–1370. <http://dx.doi.org/10.1038/nature08900>
- Nguyen, K.D., Y. Qiu, X. Cui, Y.P.S. Goh, J. Mwangi, T. David, L. Mukundan, F. Brombacher, R.M. Locksley, and A. Chawla. 2011. Alternatively activated macrophages produce catecholamines to sustain adaptive thermogenesis. *Nature.* 480:104–108. <http://dx.doi.org/10.1038/nature10653>
- Peschon, J.J., P.J. Morrissey, K.H. Grabstein, F.J. Ramsdell, E. Maraskovsky, B.C. Gliniak, L.S. Park, S.F. Ziegler, D.E. Williams, C.B. Ware, et al. 1994. Early lymphocyte expansion is severely impaired in interleukin 7 receptor-deficient mice. *J. Exp. Med.* 180:1955–1960. <http://dx.doi.org/10.1084/jem.180.5.1955>
- Price, A.E., H.-E. Liang, B.M. Sullivan, R.L. Reinhardt, C.J. Eisle, D.J. Erle, and R.M. Locksley. 2010. Systemically dispersed innate IL-13-expressing cells in type 2 immunity. *Proc. Natl. Acad. Sci. USA.* 107:11489–11494. <http://dx.doi.org/10.1073/pnas.1003988107>
- Reese, T.A., H.-E. Liang, A.M. Tager, A.D. Luster, N. Van Rooijen, D. Voehringer, and R.M. Locksley. 2007. Chitin induces accumulation in tissue of innate immune cells associated with allergy. *Nature.* 447:92–96. <http://dx.doi.org/10.1038/nature05746>
- Ricardo-Gonzalez, R.R., A. Red Eagle, J.I. Odegaard, H. Jouihan, C.R. Morel, J.E. Heredia, L. Mukundan, D. Wu, R.M. Locksley, and A. Chawla. 2010. IL-4/STAT6 immune axis regulates peripheral nutrient metabolism and insulin sensitivity. *Proc. Natl. Acad. Sci. USA.* 107:22617–22622. <http://dx.doi.org/10.1073/pnas.1009152108>
- Rothenberg, M.E., and S.P. Hogan. 2006. The eosinophil. *Annu. Rev. Immunol.* 24:147–174. <http://dx.doi.org/10.1146/annurev.immunol.24.021605.090720>
- Schipper, H.S., B. Prakken, E. Kalkhoven, and M. Boes. 2012. Adipose tissue-resident immune cells: key players in immunometabolism. *Trends Endocrinol. Metab.* 23:407–415. <http://dx.doi.org/10.1016/j.tem.2012.05.011>
- Schmitz, J., A. Owyang, E. Oldham, Y. Song, E. Murphy, T.K. McClanahan, G. Zurawski, M. Moshrefi, J. Qin, X. Li, et al. 2005. IL-33, an interleukin-1-like cytokine that signals via the IL-1 receptor-related protein ST2 and induces T helper type 2-associated cytokines. *Immunity.* 23:479–490. <http://dx.doi.org/10.1016/j.immuni.2005.09.015>
- Spits, H., and J.P. Di Santo. 2011. The expanding family of innate lymphoid cells: regulators and effectors of immunity and tissue remodeling. *Nat. Immunol.* 12:21–27. <http://dx.doi.org/10.1038/ni.1962>
- Turcot, V., L. Bouchard, G. Faucher, V. Garneau, A. Tchermof, Y. Deshaies, L. Pérusse, S. Marceau, S. Biron, O. Lescelleur, et al. 2012. Thymic stromal lymphopoietin: an immune cytokine gene associated with the metabolic syndrome and blood pressure in severe obesity. *Clin. Sci.* 123:99–109. <http://dx.doi.org/10.1042/CS20110584>
- Turnquist, H.R., Z. Zhao, B.R. Rosborough, Q. Liu, A. Castellaneta, K. Isse, Z. Wang, M. Lang, D.B. Stolz, X.X. Zheng, et al. 2011. IL-33 expands suppressive CD11b+ Gr-1(int) and regulatory T cells, including ST2L+ Foxp3+ cells, and mediates regulatory T cell-dependent promotion of cardiac allograft survival. *J. Immunol.* 187:4598–4610. <http://dx.doi.org/10.4049/jimmunol.1100519>
- Vasudevan, A.R., H. Wu, A.M. Xydakis, P.H. Jones, E.O. Smith, J.F. Sweeney, D.B. Corry, and C.M. Ballantyne. 2006. Eotaxin and obesity. *J. Clin. Endocrinol. Metab.* 91:256–261. <http://dx.doi.org/10.1210/jc.2005-1280>
- Voehringer, D., T.A. Reese, X. Huang, K. Shinkai, and R.M. Locksley. 2006. Type 2 immunity is controlled by IL-4/IL-13 expression in hematopoietic non-eosinophil cells of the innate immune system. *J. Exp. Med.* 203:1435–1446. <http://dx.doi.org/10.1084/jem.20052448>
- Voehringer, D., N. van Rooijen, and R.M. Locksley. 2007. Eosinophils develop in distinct stages and are recruited to peripheral sites by alternatively activated macrophages. *J. Leukoc. Biol.* 81:1434–1444. <http://dx.doi.org/10.1189/jlb.1106686>
- Voehringer, D., H.-E. Liang, and R.M. Locksley. 2008. Homeostasis and effector function of lymphopenia-induced “memory-like” T cells in constitutively T cell-depleted mice. *J. Immunol.* 180:4742–4753.
- Wu, D., A.B. Molofsky, H.-E. Liang, R.R. Ricardo-Gonzalez, H.A. Jouihan, J.K. Bando, A. Chawla, and R.M. Locksley. 2011. Eosinophils sustain adipose alternatively activated macrophages associated with glucose homeostasis. *Science.* 332:243–247. <http://dx.doi.org/10.1126/science.1201475>
- Yu, C., A.B. Cantor, H. Yang, C. Browne, R.A. Wells, Y. Fujiwara, and S.H. Orkin. 2002. Targeted deletion of a high-affinity GATA-binding site in the GATA-1 promoter leads to selective loss of the eosinophil lineage in vivo. *J. Exp. Med.* 195:1387–1395. <http://dx.doi.org/10.1084/jem.20020656>
- Zeyda, M., B. Wernly, S. Demyanets, C. Kaun, M. Hämmerle, B. Hantusch, M. Schranz, A. Neuhof, B.K. Itariu, M. Keck, et al. 2012. Severe obesity increases adipose tissue expression of interleukin-33 and its receptor ST2, both predominantly detectable in endothelial cells of human adipose tissue. *Int J Obes (Lond)*. Epub before print. <http://www.nature.com/ijo/journal/vaop/ncurrent/full/ijo2012118a.html>